

UNCLASSIFIED

AD NUMBER: AD0852028

LIMITATION CHANGES

TO:

Approved for public release; distribution is unlimited.

FROM:

Distribution authorized to US Government Agencies and their Contractors;
Export Control; 1 Apr 1969. Other requests shall be referred to Air Force
Materials Laboratory, Wright-Patterson AFB, OH, 45433

AUTHORITY

USAFSC ltr dtd 26 May 1972

BEST

AVAILABLE

COPY

AFML-TR-69-47

ELIMINATION OF LOW-DENSITY
INCLUSIONS IN TITANIUM ALLOY INGOTS

F. W. Wood
U.S. Bureau of Mines
Albany Metallurgy Research Center

AD852028

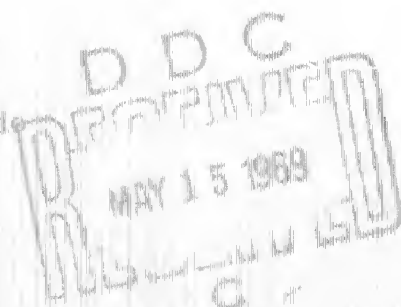
Technical Report AFML-TR-69-47

April 1969

This document is subject to special export controls and each transmittal to foreign governments or foreign nationals may be made only with prior approval of the Manufacturing Technology Division of the Air Force Materials Laboratory, Wright-Patterson Air Force Base, Ohio 45433.

attn: MATP.

Air Force Materials Laboratory
Air Force Systems Command
Wright-Patterson Air Force Base, Ohio



ACQUISITION FOR	
ORDS	WHITE SECTION <input type="checkbox"/>
DDO	DIFF SECTION <input type="checkbox"/>
ORANOMICES	<input type="checkbox"/>
DISTRIBUTION	
BY	
DISTRIBUTION/AVAILABILITY CODE:	
GEN.	ADVIS. AND/OR SPECIAL
2	

NOTICES

When Government drawings, specifications, or other data are used for any purpose other than in connection with a definitely related Government procurement operation, the United States Government thereby incurs no responsibility nor any obligation whatsoever; and the fact that the Government may have formulated, furnished, or in any way supplied the said drawings, specifications, or other data, is not to be regarded by implication or otherwise as in any manner licensing the holder or any other person or corporation, or conveying any rights or permission to manufacture, use, or sell any patented invention that may in any way be related thereto.

This document is subject to special export controls, and each transmittal to foreign governments or foreign nationals may be made only with prior approval of the Manufacturing Technology Division, Air Force Materials Laboratory. The distribution of this report is limited because the report contains technology identifiable with items on the strategic embargo lists excluded from export or reexportation under U. S. Export Control Act of 1949 (63 STAT. 7), as amended (50 U. S. C. App. 2020, 2031), as implemented by AFR 400-10, AFR 310-2, and AFSCR 80-20.

Copies of this report should not be returned unless return is required by security considerations, contractual obligations, or notices on a specific document.

BLANK PAGE

ELIMINATION OF LOW-DENSITY
INCLUSIONS IN TITANIUM ALLOY INGOTS

F. W. Wood

This document is subject to special export controls and each transmittal to foreign governments or foreign nationals may be made only with prior approval of the Manufacturing Technology Division of the Air Force Materials Laboratory, Wright-Patterson Air Force Base, Ohio 45433.

FOREWORD

This Technical Report covers work performed under Contract F33015-63-M-5002 from 1 September 1967 to 30 August 1968. The manuscript was released by the authors in January 1969 for publication.

This contract with the Albany Metallurgy Research Center (AMRC) of the Bureau of Mines, Albany, Oregon, was initiated under Manufacturing Methods Project 161-8, "Elimination of Low-Density Inclusions in Titanium Alloy Ingots". The project was administered under the technical direction of R. L. Kennard, Materials Processing Branch (MATP), Wright-Patterson Air Force Base, Ohio. Floyd W. Wood, Project Leader, Metals Processing Projects, AMRC was the principal investigator. The work was supervised by Robert A. Beall, Project Coordinator, Metals Processing Projects, and by H. Gordon Peole, Research Director, AMRC. T. T. Campbell and C. E. Muesler performed reduction-process experiments, and S. C. Schasfer and G. L. Hudley prepared titanium oxynitrides. P. A. Romanos was primarily responsible for microprobe analysis. H. H. Nalzigor substituted for the principal investigator during a 2-month absence of the latter. The entire Metals Processing Projects staff contributed in various ways.

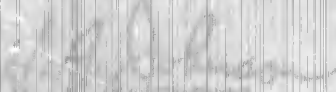
This project has been accomplished as a part of the Air Force Manufacturing Methods Program, the primary object of which is to establish on a timely basis, manufacturing processes, techniques, and equipment for use in economical production of USAF materials and components.

The program encompasses the following technical areas:

- Metallurgy - Rolling, Forging, Extruding, Drawing, Casting, Powder Metallurgy, Composites
- Chemical - Propellants, Plastics, Textile Fibers, Graphite, Fluids and Lubricants, Elastomers, Ceramics
- Electronics - Solid State, Materials and Special Techniques, Thermionics
- Fabrication - Forming, Material Removal, Joining, Components

Suggestions concerning additional Manufacturing Methods projects required on this or other subjects will be appreciated.

This technical report has been reviewed and is approved.


H. G. PEOLE

Chief, Materials Processing Branch
Manufacturing Technology Division

ABSTRACT

The problem of alpha-stabilized defects in ingots and billets of titanium and its alloys was investigated. Possible origins were considered, several naturally-occurring defects were studied, and elimination by nitrides was selected as a case needing further investigation. Nitride defects were synthesized in ingots, their nature and behavior during melting, casting, and subsequent rolling were explored, and elimination of the artificial defects was attempted by means of melting-process variations. Nitride defect seeds survived melting in three forms, each consistent with the Ti-TiN phase system if different thermal exposures during melting, solidification, and cooling are assumed. In cold-mold arc melting trials, factors that tended to alleviate ingot defectiveness were good vacuum, high arc current, remelting, and pneumatic vibration of the melts. Other variations used were unidirectional magnetic stirring and electroslag melting. Improvements obtained by varying the cold-mold practice were generally not good enough. However, reasonable preliminary success was achieved by adopting skull casting as the melting practice. More extensive evaluation of this technique is recommended.

TABLE OF CONTENTS

		<u>Page</u>
1.	INTRODUCTION	1
	1.1 The Problem	1
	1.2 Project Goals	2
	1.3 Summary of Project Accomplishments	2
2.	SOURCES OF INCLUSIONS	4
	2.1 Survey of Possible Origins	4
	2.1A Basic Rationalization	4
	2.1B Production Irregularities	10
	2.1C Materials Anomalies	14
	2.2 Examination of Defects	18
	2.3 Reduction-Process Experiments	29
3.	STUDY OF SYNTHETIC DEFECTS	33
	3.1 Preparation of Nitrides and Oxynitrides	33
	3.2 Melting and Examining Ingots With Artificial Flaws	38
	3.3 Nature and Behavior of Nitride Defects	43
	3.4 Syntheses of Other Defects	60
4.	DEFECT SURVIVAL IN MELTING	62
	4.1 Unalloyed Ingots	62
	4.2 Ti-4Al-4V Alloy Ingots	67
	4.3 Discussion	80
5.	CONCLUSIONS AND RECOMMENDATIONS	83
6.	REFERENCES	84

LIST OF ILLUSTRATIONS

Fig.		Page
1.	Defective region and alpha-stabilized reaction zone. Microprobe analysis of the small inclusions gave 5.9 to 5.3% N and less than 1% each of Al and V. Ti-6Al-4V. Originally 25X.	19
2.	Magnified view of reaction zone in Fig. 1, showing two phases. Microprobe analysis gave 5.8% V and 4.5% Al in the dark phase, and 1.5% V and 6.0% Al in the light phase. Ti-6Al-4V. Originally 400X.	19
3.	Defective region with inclusions and an alpha-stabilized zone. Ti-6Al-4V. Originally 25X.	20
4.	Two-phase structure of reaction zone in Fig. 3. Ti-6Al-4V. Originally 400X.	20
5.	Microstructure of the spongy inclusion in Fig. 3, probably β -phase, predominantly Ti_3N (epsilon phase) according to X-ray diffraction. Ti-6Al-4V. Originally 400X.	21
6.	Elongated defect with a reaction zone. Ti-6Al-4V. Originally 25X.	21
7.	Two-phase reaction zone shown in Fig. 6. Ti-6Al-4V. Originally 400X.	22
8.	Small alpha-encased defect. Ti-6Al-4V. Originally 25X.	22
9.	Defect with inclusions and reaction zone. Ti-6Al-4V. Originally 30X.	23
10.	One of the spongy inclusions shown in Fig. 5. Microprobe analysis gave about 7.5% N. Ti-6Al-4V. Originally 400X.	23
11.	Defect with extensive alpha-stabilization and crack. Ti-6Al-4V. Originally 25X.	24
12.	Elongated and cracked defective region. Ti-6Al-4V. Originally 25X.	24

LIST OF ILLUSTRATIONS (Continued)

<u>Fig.</u>		<u>Page</u>
13.	Defect with a limited reaction zone. Ti-6Al-4V. Originally 25X.	25
14.	Defective region with spongy inclusions. Ti-6Al-4V. Originally 25X.	25
15.	Spongy inclusion of Fig. 14. Ti-6Al-4V. Originally 400X.	26
16.	Defect with unusually large inclusion fragment. Ti-6Al-4V. Originally 25X.	26
17.	Defect and inclusions. Microprobe analysis gave about 5.7% Al and 2.1% Sn in the reaction zone. Ti-5Al-2.5Sn. Originally 50X.	27
18.	A spongy inclusion shown in Fig. 17. Microprobe analysis gave 11.9 to 14.8% N, 1.5 to 5.2% Sn, and less than 1% Al. Ti-5Al-2.5Sn. Originally 100X.	27
19.	"Basket-weave" alpha-stabilized band, ultrasonically detectable. Ti-3Al-2.5Sn. Originally 50X.	28
20.	Bright-etching band. Ti-5Al-4V. Originally 50X.	28
21.	Qualitative suggestions for phase features of an isothermal section, at about 1,500° C, in the Ti-TiC-TiN system.	36
22.	Specimen 937U. 3 sec. etch, oblique light. Detail at tip of type I defect. Originally 25X.	45
23.	Specimen 937L. Microprobe back-scattered electron image. Type I defect and basket-weave reaction zone. Originally 150X.	45
24.	Specimen 937U. Microprobe back-scattered electron image. Type I defect and basket-weave reaction zone. Originally 150X.	46
25.	Specimen 937U. Microprobe X-ray pattern of nitrogen, corresponding to Fig. 24. Originally 150X.	46

LIST OF ILLUSTRATIONS (Continued)

	<u>Page</u>
26. Specimen 937D. 3 sec. etch, oblique light. Detail of type II defect. Originally 25X.	47
27. Specimen 951B. 3 sec. etch, oblique light. Type III defective region. Originally 35X.	47
28. Specimen 951B. 3 sec. etch, oblique light. Another type III defective region. Originally 25X.	48
29. Specimen 951B. Microprobe back-scattered electron image of type III defect. Originally 250X.	48
30. Etched ingot section showing appearance of type III defective regions.	49
31. Type I defect in unalloyed plate 948B after rolling at 1,000° C. Polished with 600 grit SiC, HF-HNO ₃ etch. Originally 25X.	54
32. Two small type I defects in unalloyed plate 948E after rolling at 1,000° C. Polished with 600 grit SiC, HF-HNO ₃ etch. Originally 12X.	54
33. Type II defect in unalloyed plate 948B after rolling at 1,000° C. Polished with 600 grit SiC, HF-HNO ₃ etch. Originally 25X.	55
34. Type III defect in unalloyed plate 948B after rolling at 1,000° C. Polished with 600 grit SiC. Not etched. Originally 12X.	55
35. Type I defect in unalloyed plate 947A after rolling at 850° C. Polished with 240 grit SiC. Not etched. Originally 12X.	56
36. Type II (bright) and type III (dark) defects in unalloyed plate 948A after rolling at 850° C. Polished with 240 grit SiC, HF-HNO ₃ etch. Originally 6X.	56
37. Anomalous type II defect in unalloyed plate 940A after rolling at 850° C. Polished with 600 grit SiC. Not etched. Originally 12X.	57
38. Ti-TiN phase system.	58

LIST OF ILLUSTRATIONS (Continued)

<u>Fig.</u>		<u>Page</u>
39.	Ingot of unalloyed Ti, melted at 2,200 amp. in dynamic vacuum with defects induced artificially.	65
40.	Ingot of unalloyed Ti, melted at 2,700 amp. in dynamic vacuum with defects induced artificially.	65
41.	Ingot shown in Figure 39, after etching.	66
42.	Ingot shown in Figure 40, after etching.	66
43.	Typical 5-inch arc-melted ingots of Ti-6Al-4V alloy, containing artificial defects, as-cast condition.	70
44.	Six-inch electroslag-melted ingot to which defect seeds were added.	71
45.	Some defective ingots after cutting and polishing for evaluation.	72
46.	Close-up view of a skull-cast ingot apparently free of types I and II alpha-stabilized defects.	73
47.	Etched cross section of ingot SA 26206.	74
48.	Etched cross section of ingot SA 26220.	75
49.	Etched cross section of ingot SA 26209.	76
50.	Etched cross section of ingot SA 26257.	77
51.	Etched cross sections of ingots SA 26412 (left) and SA 26421 (right).	78
52.	Etched cross section of ingot SA 26424.	79

LIST OF TABLES

		<u>Page</u>
I.	Analyses of Lumps From Titanium Sponge Selected for Odd Appearance or Known Impurity.	15
II.	Chemical Compositions Reported for Some Selected Titanium Sponges.	17
III.	Conditions for Nitrogen Contamination of Magnesium Reductant.	31
IV.	Distribution of Nitrogen in Titanium Sponge Prepared with Contaminated Reductant and/or Reacting Gas.	32
V.	Residual Nitrogen (wt. %) After Fusion of TiN.	33
VI.	Composition and Cubic Cell Size for Some Single-Phase Ti (C, N).	37
VII.	Vendor's Analyses of Ti Sponge.	38
VIII.	Defect Seeding of Unalloyed Electrode Bars.	40
IX.	Defect Seeding of Ti-6Al-4V Electrode Bars.	41
X.	Nitrogen Distribution in Type I Defects.	50
XI.	Some Radiographic Parameters for 0.3 Angstrom X-rays.	51
XII.	Unalloyed Ingots.	63
XIII.	Defectiveness Scores for Unalloyed Ingots.	64
XIV.	Ti-6Al-4V Alloy Ingots.	68
XV.	Defectiveness Scores for Ti-6Al-4V Ingots.	69

BLANK PAGE

ELIMINATION OF LOW-DENSITY INCLUSIONS IN TITANIUM ALLOY INGOTS

1. INTRODUCTION

1.1 The Problem

For several years, during development and commercial production of titanium and its alloys, many investigators, producers, and users have noticed that arc-melted ingots or products therefrom contained localized defective regions that are not detectable with certainty by regular ultrasonic or radiographic tests. The defects frequently are described as having a low density, but this is correct only in the sense of radiographic transparency. Most of the flaws include hard alpha-stabilized regions, many of them enclosing some extra phase other than alpha or beta titanium. The alpha-stabilized zones have a relatively coarse structure, but slightly smaller lattice parameters than normal alpha-phase titanium. Increased phases are brittle, and the entire defective regions tend to be susceptible to corrosion. In any case, the defect sites are stressed regions that may rupture or crumble, and initiate cracks during deformation, and those that are detected ultrasonically or radiographically are usually found because of crack or void formation. Occasionally, one of the flaws will be discovered because of metal failure during a manufacturing or testing process. Any defects, with or without cracking, that are not detected are bound to cause a weakness of the finished part.

The defects are rare by some standards. They have been present in about two to four percent of the ingots produced over an extended time period. However, over short increments of time, the ratio is quite erratic. Discoveries of defects seem to be grouped in time, and significant periods elapse without the appearance of the subject flaws.

A serious effort to eliminate the problem is amply justified by the chance that a single undetected inclusion could, in some uses, cause a catastrophic failure costing millions of dollars in direct material loss, and jeopardizing human lives. More typically, losses amounting to tens of thousands of dollars have actually occurred.

1.2 Project Goals

The purposes of this work have been to investigate possible origins of alpha-stabilized inclusions in primary metal production, and to attempt to reduce the occurrence or survival of the defects by means of process modifications.

In the language of the Contract Work Statement:

"1. The purpose of this program is to investigate and improve titanium alloy ingot consolidation practice in order to eliminate the low-density inclusions associated with the Ti-6Al-4V alloy.

2. The specific objectives of this program are:

- a. To determine the sources of the low-density inclusions and to identify these defects.
- b. To define the conditions necessary for producing 'alpha segregation' in titanium alloys, in particular, Ti-6Al-4V."

1.3 Summary of Project Accomplishments

Arc-melted ingots of titanium alloys or products therefrom sometimes contain localized defective regions that are alpha-stabilized and not detectable with certainty by regular ultrasonic or radiographic tests. Possible origins of the alpha-stabilized defects in primary metal production were investigated, and elimination of the defects was attempted by means of melting-process variations.

Logically, the alpha-stabilized defects are probably caused by refractory lumps of oxygen- or nitrogen-rich material that fail to melt completely during ingot production. In operations for the production of titanium, there are more opportunities for contamination by oxygen than by nitrogen, and oxygen contamination is actually found more often in sponge products. However, at the basic melting temperature and density, nitrogen contamination is more apt to survive melting without dissolving. Furthermore, significant nitrogen enrichment does occur. It has been observed in commercial products and demonstrated in experiments. Finally, nitrogen is the impurity most often associated with actual defects in billets and ingots.

Nitrogen-rich flaws, similar to naturally-occurring defects, have been synthesized and studied in arc-melted ingots of unalloyed and Ti-6Al-4V compositions. The defects in as-cast metal are of three types, with different degrees of coherency. Type I defects contain incoherent inclusions with one or more brittle phases. Type II defects are coherent inclusions of microscopically separated, hard, alpha-stabilized phases. Type III defects also are coherent, but phases are separated on a microscopic scale that makes it difficult to characterize the phases. Proximate to type III defects, lattice expansion, hardening, and corrosion susceptibility are noticeable in the host structure, however. Useful changes do not appear in defective regions after 3-hour annealing tests at 1,100° C. Most features of the three types of defects are explainable, with the help of microprobe analyses and knowledge of the Ti-TiN system, by considering the probable progress of dissociation, dissolution, and solidification.

Preliminary experiments on the effects of rolling metal with artificial defects indicate that the type I defects respond by crumbling and are obviously detrimental. The responses of type II and III defects are more subtle, and although both types can persist to cause imperfections in products, it is not yet clear, without more careful study of their behavior and consequences, that they must be eliminated.

In the course of arc melting experiments, several factors were varied and their effects on the survival of artificial defects were observed. Twenty-six cold-mold ingots were produced by a consumable-electrode arc-melting technique. Twelve ingots were unalloyed, fourteen were of Ti-6Al-4V alloy. Seventeen ingots were first melts, nine were remelts. Eleven ingots had 3-inch diameters, one had a 4-inch diameter, and fourteen had 2-inch diameters. Conditions that seemed to limit the number and severity of surviving defects were high arc current, good furnace vacuum, a rapid melting rate, repeated melting, and mechanical vibration of the molten metal. Slow melting and the use of unidirectional magnetic stirring led to poorer ingot quality. Besides the arc melts, two ingots were melted under a calcium fluoride electroslag — one a 3-inch-diameter melt of unalloyed Ti, the other a 6-inch-diameter melt of Ti-6Al-4V — and they also were quite defective. The best apparent success in dissolving nitride defect seeds resulted when 4-inch-diameter ingots were poured by the cold-mold skull-casting method. Three of these were produced — one of them a first melt, two of them remelts, and all three of Ti-6Al-4V alloy.

The work under this contract has indicated that many alpha-stabilized defects are of a refractory nitrogen-rich variety. To date, the best chance for eliminating these and other similar defects seems to be in using skull casting as a first melting procedure in a two-stage melting sequence. However, this approach has not been thoroughly tested, and economic implications might be serious. An approach that was not investigated under this contract is the use of trace additives, such as yttrium or some of the lanthanide metals, to encourage dissolution of refractory phases.

2. SOURCES OF INCLUSIONS

2.1 Sources of Possible Origins

2.1A Basic rationalization

One of the first decisions made was whether the "segregation" occurred by a process of phase separation from solution or by a process of non-solution. A relevant factor was the observation that many of the defects are unusually large for precipitated nodules or other forms of separated phases. Another consideration was the fact that defects of essentially the same type have been found in a variety of alloy phase systems besides the Ti-6Al-4V alloy, including some alloys of titanium's sister metal zirconium. It would be difficult to explain the prevalence of similar phase separation processes in widely different equilibrium systems. It had also been noticed by various observers that there was a tendency for alpha-stabilized inclusions to occur in lower, early-freezing parts of ingots instead of in metal that is known to freeze later and slower. This seemed to imply that defect formation was favored by short thermal cycling. Finally, to experienced metallographers, the defects simply did not look like examples of phase separation. They looked like partially unmelted or incompletely dissolved material instead. All of these factors favored the idea of a non-solution process and no good reasons for behaving otherwise were recognized, so subsequent work was based on the premise that the defects resulted from the presence of refractory particles or lumps.

Having decided to look for refractory materials, it was appropriate to consider binary compositions. The outline below summarizes information about phases that contain titanium as a component, and that are known to have melting temperatures above 1,660° C, the melting point of titanium (29) ^{1/}.

^{1/} Underlined numbers in parentheses are references.

Outline of
Some Refractory Phases in Titanium Systems

Based on References
(3, 9, 14, 16, 17, 21, 24, and 36)

I. Binary and Pseudo-binary Alloys Containing Ti

A. Solid-solution type

- | | |
|----------|----------|
| 1. Ti-V | 4. Ti-Mo |
| 2. Ti-Cr | 5. Ti-Ta |
| 3. Ti-Cb | |

B. Peritectic type

- | | |
|--------------------------|--|
| 1. Ti-TiB ₂ | 6. Ti ₅ Si ₃ -Si |
| 2. Ti-Ti _x C | 7. Ti-W |
| 3. Ti-Ti _x N | 8. Ti-Re |
| 4. Ti-Ti ₄ O | 9. Ti-Ti ₅ Re ₂₄ |
| 5. Ti ₄ O-TiO | 10. TiPt ₃ -Pt |

C. Eutectic type

- | | |
|---|---------------------------------------|
| 1. TiC-C | 5. Ti-Ti ₅ Si ₃ |
| 2. TiO-Ti ₂ O ₃ | 6. TiSi-Si |
| 3. Ti ₂ O ₃ -Ti ₃ O ₅ | 7. Ti-TiPt |
| 4. Ti ₃ O ₅ -TiO ₂ | 8. TiPt-TiPt ₃ |

II. Binary Compounds and Intermediate Phases

- A. Ti₂B Stable from 1,800° C to 2,200° C -
formed by peritectic reaction at the
upper temperature - narrow composition
range near 10 w/o B - tetragonal structure
(a : b : c = 1 : 1 : 1.53, c/a = 0.743)

- B. TiB Stable up to $2,060^{\circ}C$ - formed by peritectoid reaction (Ti_2B and TiB_2) - narrow composition range near 15.5 w/o B - orthorhombic structure type B37 isotypic with FeB (a : 6.12A, b : 3.06A, c : 4.56A) (D_{2h}^{16} - P6mm), 8 atoms/unit cell - density 5.1 g/cc - covalently bonded interstitial compound with metallic character.
- C. TiB_2 Stable up to $2,790^{\circ}C$ - broad composition range, 30 to 34 w/o B - hexagonal structure, type C 32 isotypic with AlB_2 (a : 3.03A, c : 3.22A, c/a : 1.06) (D_{6h}^{18} - P6/mmm) 8 atoms/unit cell - density 4.45 g/cc - bonding mainly covalent with considerable metallic character.
- D. Ti_2B_5 Stable up to $2,090^{\circ}C$ - about 36 w/o B - hexagonal structure, W_2B_5 type (a : 2.98A, c : 13.98A, c/a : 4.69) 10 atoms/unit cell
- E. TiB_{12} Apparently stable up to $2,300^{\circ}C$ (m. p. of B) - about 73 w/o B - structure unknown, probably an arrangement of Kasper icosahedra on a close packed cubic or hexagonal lattice
- F. TiC Stable to $3,140^{\circ}C$ - broad composition range, 11 to 20 w/o C - fcc structure, type B1 isotypic with NaCl (a : 4.32A) (O_h^F - Fm3m) 8 atoms/unit cell - density 4.33 g/cc - interstitial compound, probably with strong d^4sp^3 hybrid metallic bond
- G. Ti_4N Stable from $1,600^{\circ}$ to $2,350^{\circ}C$ - formed by peritectic reaction - apparently a line compound at 6.8 w/o N - alpha Ti structure, bcc
- H. Ti_6N Stable to above $1,590^{\circ}C$ (Note: most reports indicate about $1,050^{\circ}C$ max.) - formed by peritectoid reaction (Ti_2N and Ti_8N_2) - apparently a line compound at 9 w/o N - antiferite, complex tetragonal structure (a : 4.92A, c : 5.61A, c/a : 1.05)

- J. TiN Stable to 2,950° C - broad composition range, 10 to 24 w/o N (lower limit corresponds approx. to Ti_3N_2) - fcc structure, type B1 isotypic with NaCl (a : 4.24Å) ($O_h^3 - Fm\bar{3}m$) 8 atoms/unit cell - density 5.3 g/cc - strong metallic component of covalent bond
- J. Ti_4O Stable to 1,900° C - broad composition range, 0 to 14.5 w/o O - alpha (hcp) solid solution of O in Ti
- K. TiO Stable to 1,770° C - formed by peritectic reaction - possibly a line compound at 25 w/o - fcc structure, type B1 isotypic with NaCl (a : 4.15Å) ($O_h^3 - Fm\bar{3}m$) 8 atoms/unit cell - density 4.93 g/cc
- L. Ti_2O_3 Stable to 1,900° C - congruently melting line compound at 33.4 w/o O - hexagonal structure, alpha Al_2O_3 type (corundum) (a : 5.15Å, c : 13.81Å, c/a : 2.64)
- M. Ti_3O_5 Stable from 1,200° to 1,850° C - congruently melting line compound at 35.7 w/o O - orthorhombic structure, type C 49 (a : 3.75Å, b : 8.47Å, c : 9.73Å) ($C_{2h}^{17} - Cmc21$)
- N. TiO_2 Stable to 1,850° C - moderately broad composition range, 38 to 40 w/o O - tetragonal structure, type C4 (a : 4.58, c : 2.95, c/a : 0.64) ($D_{2h}^{14} - P4_2mm$) - density 4.2 g/cc
- O. Ti_3Si_3 Stable to 2,120° C - narrow composition range, almost a congruently melting line compound, near 26 w/o Si - hexagonal structure, type $D5_3$ isotypic with Mn_3Si_3 (a : 7.41Å, c : 5.15Å, c/a : 0.69) ($D_{6h}^3 - P6_3/mcm$) 16 atoms/unit cell
- P. $TiSi$ Stable to 1,760° C - formed by peritectic reaction - line compound at 37 w/o Si - orthorhombic structure, type B27 isotypic with FeSi (a : 3.61Å, b : 4.96Å, c : 5.48Å) ($D_{2h}^{16} - Fm\bar{3}m$) 8 atoms/unit cell - metallic-covalent bonding - density approx. 4.9 g/cc

- Q. Ti_5Re_{24} Stable to 2,750° C - formed by peritectic reaction - line compound at 95 w/o Re - bcc structure, type A12 isotypic with alpha Mn (a : 9.59kX) (T_d^B - 148 m) 58 atoms/unit cell
- M. TiPt Stable to 1,830° C - narrow composition range near 30 w/o Pt - structure unknown
- S. $TiPt_3$ Stable to 1,950° C - congruently melting line compound at 92.5 w/o Pt - fcc structure, type L1₂ isotypic with Cu_3Au (a : 3.92A) (C_h^1 - Pm3m) 4 atoms/unit cell

Notice that the compounds TiB_2 , TiC, TiN, and Ti_5Re_{24} are especially refractory, each melting at a temperature above 2,700° C. Measurements (35) have indicated that typical "average" temperatures in molten pools of titanium during arc melting are about 2,000° C or 2,100° C, and calculations can be made (38) to suggest a maximum temperature near 2,600° C for the case of titanium.

However, refractoriness is not the sole criterion for suspecting that a contaminant may have the capability of causing low-density inclusions. In particular:

(a) In combination with titanium, the contaminating phase must tend to stabilize the alpha polymorph (hexagonal).

(b) As mentioned previously, the defects are usually found low in ingots. This probably means that the contaminating phase sinks to the bottom of the molten pool, and to do this the contaminant must have a specific gravity somewhat greater than 4.5 g/cc, the density of titanium.

(c) There must be a reasonable chance for the contamination to be introduced during the normal course of metal production. The general susceptibility of titanium to detrimental contamination has forced producers to institute rather stringent quality control procedures, and it is not likely that a completely extraneous material would go undetected. Surely, flukish exceptions do occur, but it is probable that a problem as chronic as the alpha-stabilized defects is caused by contamination in an unobtrusive form - buried inside lumps of sponge metal, for example.

Now, resuming consideration of the refractory phases, none of the solid solution alloys listed are alpha-stabilized, and of course they are not the sort of structurally incoherent phases that are involved anyway. Tungsten or rhenium contamination causes inclusions that are well known and readily detectable as radiographically dense. They definitely are not suspect in the subject instance. Carbon is not an alpha stabilizer, and in fact it has very limited solid solubility in either alpha or beta titanium so that any extensive reaction zone around carbide inclusions would be characterized by a peritectic or peritectoid structure. Silicon and boron contamination probably can be excluded from consideration because the resulting phases have low specific gravities. And finally, platinum (as well as rhodium and boron, already concluded on other grounds) is simply not likely to get into the titanium production stream with any significant frequency. Thus, the contaminants that have the best chance to cause the alpha-stabilized defects are oxides and nitrides. And of these, the nitrides are more refractory and more dense.

Actually, a contaminant that causes an alpha-stabilized inclusion need not be a binary phase. But as far as is known, the multicomponent phases that satisfy the necessary conditions involve basically the same components as the binary phases considered. Furthermore, the greater the number of components that must participate in a reaction, the less likely the reaction is. Titanium oxynitrides, titanium carbonitrides, and even titanium oxycarbonitrides are nevertheless among possibilities.

When low-density inclusions are found in ingots, they contain titanium as a component, but this does not mean that the contaminating phase necessarily contained titanium before melting. It only means that the contaminating phase must be to some degree miscible with titanium, and the product of interaction must be relatively refractory. This sort of conjecture leads to consideration of compounds like AlN, VN, MgO, and Al₂O₃, and the systems Ti-Al-N, Ti-V-N, Ti-Mg-O, and Ti-Al-O. Unfortunately, these materials, as well as the systems mentioned in the preceding paragraph, have not been studied thoroughly enough to provide a basis for properly evaluating their role as sources of alpha-stabilized defects.

2.1B Production Irregularities

Current practices in the production of primary titanium metal were surveyed by means of discussions with knowledgeable scientists and engineers, and by means of production-plant visitations. This sort of approach is necessarily restricted by proprietary factors, but a surprising degree of cooperation was obtained from most producers and from many individuals and groups engaged in related activities. Some information was conveyed confidentially. The direct purpose of the review was the discovery of ways in which metal might be contaminated by refractory materials.

It is beyond the scope of this report to present any comprehensive description of production processes. Nonproprietary aspects of sponge production are discussed elsewhere (4, 5, 15, 20, 22, 34). Until recently, when a major producer partially adopted a proprietary fused-salt electrolytic process, practically all of the commercial production of titanium was by metallic reduction of the tetrachloride. Either magnesium or sodium can be used as the reductant. The basic reactions are:

for reduction by Mg -



$$\Delta F = - 74.9 \text{ kcal/mol at } 1,100^\circ \text{ K}$$

for reduction by Na -



$$\Delta F = - 82.7 \text{ kcal/mol at } 1,100^\circ \text{ K}$$



$$\Delta F = - 63.7 \text{ kcal/mol at } 1,100^\circ \text{ K}$$

These reactions are carried out in steel (usually stainless) vessels under the protection of an inert gas and/or vacuum. The product is sponge titanium mixed with residual salt. Part of the salt is separated mechanically and the remainder is removed by vacuum distillation or by leaching in water or acid.

Mainly because of lower cost, leaching is commonly used in domestic production. The leaching must be followed by a drying operation, normally in vacuum. Any large lumps are crushed or sheared, fines are screened out, a magnetic separation is used, the sponge is sized and graded, and on the basis of appearance or analytical experience, portions suspected of being impure are rejected. The remaining metal is then ready for consolidation.

The usual procedure for consolidation begins with cold compaction of the sponge into bars or bricks. The compacts are welded together into the form of an electrode, using some variation of inert-gas welding, and an ingot is formed by consuming the electrode with an electric arc and drawing the metal in a water-cooled copper crucible. One or more of the ingots resulting from the first melting, joined together if necessary, are used as an electrode for remelting in a similar manner. It is usually in the forging of such an ingot that inspections reveal the presence of low-density inclusions. At least one and often both of the melting steps are accomplished in vacuum. If vacuum is not used, an inert gas must be. Melting in vacuum is most effective in removing volatile impurities that may remain, while melting in inert gas, superficially at least, produces a smoother and cleaner ingot sidewall.

If an alloy is desired, the requisite additions are commonly made in elemental or master-alloy form to the sponge compacts as they are prepared for first melting. For most alloys, but not all of them, alloy homogeneity is improved by vacuum melting rather than inert-gas melting.

The processes briefly described above, together with their inherent features, comprise a complicated and sensitive sequence. There are many chances for error, both mechanical and human. Indeed, irregularities do occur and they are known to cause contamination. However, the instances are usually made obvious by deviations of control parameters, or by routine testing and examination of the products. In such cases, the metal producers conscientiously reject metal if necessary to assure final quality. Nevertheless, alpha-stabilized defects persist, so it is suspected that they are caused by more subtle process irregularities. Several possibilities were conceived early in the progress of this project.

Titanium is especially sensitive to contamination by air or water when the metal is at an elevated temperature during reduction of the chloride, welding of electrodes, and melting. Major contamination of this sort is of the obvious type mentioned above. But there is also a risk of small undetectable

leaks or other failures. For example, a pin-hole leak in a welded seam of a reductor-reaction vessel might cause very localized contamination that could go undetected, or an inert-gas-shielded welding operation that appears to be going well might actually be admitting just enough air to the weld zone to be detrimental, or if a single lump of leached sponge was passed on without being completely dry all the way through, it might form a kernel of contaminants during subsequent welding or melting. During magnesium reduction, it is necessary to bleed off excess magnesium chloride that is formed, and air might be admitted when the system is tapped. In fact, the possibilities are so numerous that it is disturbing. It should be noted, however, that water and air are sources primarily of oxide contamination. Decomposition temperatures for titanium dihydride are about 1,050° K at 1 atm. pressure, and about 520° K at 0.01 atm. pressure (32). Thus, hydrogen degases from solutions of molten titanium with ease. The free energies of formation for TiO₂, TiO, TiN, and TiH₂ respectively are - 178.0, - 98.9, - 55.0, and + 2.7 kcal/mol at 1,100° K, and - 212.4, - 116.9, - 78.9, and - 25.1 kcal/mol at room temperature (32, 37). Thus, oxidation is strongly favored at the expense of nitride and hydride. This preference also persists in vacuum (13). The bulk diffusion of nitrogen in titanium is, however, more rapid than that of oxygen (35), and there can be nitrogen penetration beneath a surface layer of oxide. Also, if carbon is available to react with the oxygen, the titanium is free to react with nitrogen. In fact, a way of preparing TiN is by carbon reduction of an oxide in the presence of a source of nitrogen (18).

Even if all enclosures are leak-free, the welding operation is enclosed, and other chances of introducing contamination from the outside are eliminated, the risk of contamination due to internal sources is serious. It is well known (22, 23, 33) that the first metal formed as a product of a chloride-reduction reaction scavenges or getters residual air in the system, any dirt, grease, or other contamination on the chamber walls, and impurities contained in the reductant. Most of the metal contaminated in this way forms early in the reduction cycle and either nucleates on or settles to steel surfaces in the lower part of the reaction vessel, so that it is contaminated by the steel components as well as by the other impurities. This metal is recognized by producers as being impure and they separate it for use mainly as a ferro-alloy additive. Reductant added after the reaction is underway may, however, contain additional impurities and afford an opportunity for impurity particles to form at other locations. Furthermore there is some chance that a few small pieces of the ferro-grade material occasionally become mixed with the better grades.

The scavenging of residual air or general dirt is primarily by another way of introducing oxide contamination. Oxides, including MgO, might occur in reductant metal too, but the getting of reductants is especially suitable because it is a good possibility for introducing nitride contamination. If appropriate nitrides are present in the reductants, the following side-reactions are conceivable:



$$\Delta F = - 101.4 \text{ kcal/mol at } 1,100^\circ \text{ K}$$



$$\Delta F = - 202.4 \text{ kcal/mol at } 1,100^\circ \text{ K}$$

The second of these reactions is seriously qualified and the free-energy change is given only as an inequality because free Na_3N dissociates at 423° K . However, it may be that some equilibrium composition of the compound is stable in solution with Na at higher temperatures. Comparison of the free-energy changes immediately above and on page 10 shows that, under equilibrium conditions at least, the formation of TiN is favored over the formation of pure Ti.

Following the reduction process, as the sponge metal is removed from the reaction vessel, crushed, sheared, graded, blended, or otherwise handled, there are opportunities for igniting or overheating the metal. This is another source of oxides. Again, the incidents do occur, they are usually obvious, but small amounts of contaminated material might be passed on inadvertently.

The final source of low-density inclusions to be suggested is contaminated alloy additives. A variety of refractory impurities may be added this way, depending on the alloy being produced, except that oxides and nitrides are still most suspect. In the particular case of the Ti-6Al-4V alloy, VN, AlN, VO_2 , V_2O_3 , Al_2O_3 , and their complex combinations are among possibilities. It has been reported (25) that VN is more soluble when dissolved in TiN than when it is free.

The survey of operations and accumulation of information, accomplished as part of this investigation, have failed to discount any of the suggestions reviewed above. In fact, it seems almost certain that alpha-stabilized defects have been caused in specific instances in each of the ways proposed. In various cases, proprietary investigations of processing history have plausibly shown circumstantial associations of defects with faulty welding practices, particular master alloy batches, lax practices in reductant purification, and the sponge production sequence used. In the latter connection, there have been inconclusive indications that sodium reduction, electrolytic reduction, and vacuum distillation each tends to reduce the occurrence of large defects. However, no combination of practices has avoided the defects completely, and the variations have included crushing of master alloys to be sure that any refractory impurities added in that way are finely divided, and changes from gas-shielded welding to totally enclosed welding. Zirconium alloy producers have even used electron-beam welding. And it is again relevant that more than one alloy is involved. Nevertheless, the alpha-stabilized defects keep pepping up.

2.10 Materials anomalies

A third approach to the matter of sources of low-density inclusions was an attempt to determine what impurities are actually present as refractory concentrations in sponge metal and reductant metal.

Various lots of commercial-grade titanium sponge were sorted by hand, and discolored or otherwise suspect lumps were selected for analysis. Samples of some extra-grade titanium were also analyzed. Results are summarized in Table I. About half of the specimens, representing half a ton or so, sample jars, resulted from the complete piece-by-piece sorting of about 200 lbs. of various kinds of sponge. The rest of the specimens were obtained less systematically by casual grab-sample inspection.

The technical literature contains little quantitative information of the sort shown in Table I. Only one paper of real relevance has been discovered [1], and Table II is information extracted from that source.

The trends that seem to emerge from these compilations are that refractory concentrations of either oxygen or nitrogen, but especially oxygen, can be found in titanium sponge, and that discoloration is not a reliable criterion for selecting the refractory lumps. In general, the worst oxygen and nitrogen concentrations correspond to sponge that is a benign shade of

TABLE I. - Analyses of Lumps From Titanium Sponge Selected for Odd Appearance or Known Impurity 1/

Description	N	O	Other
<u>Mg-reduced, vacuum-distilled:</u>			
Blue-black	47		
Orange spots	17		
Olive green	32		
Blue-black, rounded	35		TiO ₂ 2/
White crust found on low-oxygen sponge (cut 600 ppm) after extended storage.			
High-density lump with extra bright luster			
Dark red	400	1275	VAI ₃ and V ₅ Al ₃ 2/
Light grey	78	2.6%	
Bluish purple/gold	104	760	
Dark grey	73	2700	
Gold	720	1545	
Tan	223	477	Possibly some Fe-Ti oxide 2/ TiN X-ray pattern evident in blue stain.
Red/purple-blue			
<u>Mg-reduced, leached:</u>			
Grey-blue, rounded			Expanded Ti lattice, probably interstitial solution 2/
<u>Na-reduced, leached:</u>			
Grey-black			Ib.
Blue-gold, dense platelets	45	1.03%	As above, but also X-ray pattern of Mg ₂ Ti ₆
Orange/black spots	48	2.83%	Expanded Ti lattice (interstitial solution), 2/ Fe ₂ O ₃ , and other unidentified compounds 2/
Grey/white tan	56	2970	310 Fe, 140 O

(Continued)

TABLE I - Analysis of Zones From Titanium Steels Deformed for Cold Appearance
 of Phase Boundary 1/ (Continued)

Description	N	O	Cbar
<u>Electronically reduced</u> Gold (0/100)			
<u>Ferro-silide</u> (dark grey) big-rectangle	1400	1.46%	High Al, Cr, Fe, Mg, Mn, Ni, Si
Metallic lump from plate	750	2.07%	Fe > 0.5%, high Al, Ca, Cr, Mg, Ni, Si, Sn
Plate near lump, grey	5060	6.56%	Fe > 0.5%, Mg > 0.5%, high Al, Ca, Cr, Ni, Si, Sn, V
Fragile plate, grey			Expanded Ti lattice (interstitial solution) plus unidentified compound with (Ti ₃ Mo ₇) Si ₂ -type structure 2/
Brittle lump, dark grey			15 to 25 % α / γ solid solution of interstitial O and/or N 2/
<u>Not analyzed</u> Gold/orange/blue-grey	80	7200	Fe 1.3%, high C, Si, Cr, Ni

1/ All values in ppm unless otherwise noted.
 2/ Indicated by X-ray.

TABLE II. - Chemical Compositions Reported for Some Selected Titanium Sponges ^{1/}

<u>Description</u>	<u>N</u>	<u>O</u>	<u>H</u>	<u>Fe</u>	<u>Si</u>	<u>Cl</u>
Oxidized, yellow	2,200	4,400	100	300	400	600
Oxidized, bluish-violet	7,500	1.6%	1,000	100	400	1,000
Oxidized, greyish-white	4.76%	2.17%	100	100	400	300
Dark grey	570	1.85%	100	3,400	1,000	1,000

^{1/} All values in ppm unless otherwise noted.

grey. Brighter colors appear to be quite superficial and primarily reveal optical conditions. The rejected ferro-grade sponge is, of course, very impure, and if any of it is mixed with sponge for primary titanium production, it could be a source of inclusions.

Despite one authoritative denial, inquiries about inclusions and segregates in magnesium metal have revealed a prevalence of opinion and evidence that heterogeneities are present, at least in some cases. This is confirmed to some extent in technical literature (7, 19, 20). Beyond this, the situation is confused by proprietary secrecy. It is not clear what the inclusions are or what is done about them. Some ten years ago, it was reported (19) that molten magnesium was chemically purified of iron by a process (7) that is also capable of reducing oxygen and nitrogen contamination (33). However, as nearly as can be learned, the method is no longer practiced. In fact, no specific evidence was obtained that any precautions are taken against refractory particles in magnesium. Reducant-grade ingots are generally cast directly from electrolytic cells.

As a part of this investigation, two reductant-grade magnesium ingots with slightly different histories were given a very cursory examination. Near top center, each had a shrinkage region containing cracks and small black inclusions. One also had a black scab-like crust on the exposed surface of the shrinkage region. Analysis of the black material by X-ray diffraction indicated that the primary constituent was MgO and that MgO was a secondary constituent. It is, however, difficult to avoid surface oxidation of magnesium samples and the oxide may not really be part of the black material. A metal analysis of a macro-sample of some of the dirty metal revealed about 900 ppm of nitrogen, but the same method showed only 10 ppm of nitrogen in clean magnesium.

Sodium metal destined for use in $TiCl_4$ reduction is also produced electrolytically. The standard practice in this case is to pass the molten metal through a screen and two stages of filtration after the electrolytic reduction is done and before the sodium is used as a reductant. Thus, only impurities thoroughly dissolved in the sodium, or those added in final handling are apt to reach the $TiCl_4$ -reduction reactor.

2.1 Examination of Defects

Clues to the sources of low-density inclusions can result from inspections of the defects themselves. Characterization of the defects was the primary objective of a related Air Force Contract F33615-87-C-1737 at another laboratory (13). However, in the course of work being reported here, some examples of defects became accessible for examination. The opportunities were welcomed.

Figures 1 through 20 are selected micrographs illustrating defects found in commercial ingots. In each case, the defect was found and the specimen removed only after some forging had been done on twice-melted metal.

In addition to optical metallography, microprobe analysis was applied to fifty specimens representing flaws in double-melted and forged metal, and to five specimens representing once-melted, as-cast metal. All of the specimens came from commercial ingots. All but two specimens came from Ti-6Al-4V alloy metal. One of the exceptions came from remelted Ti-7Al-3Mo alloy, and another from remelted Ti-3Al-2.5Sn alloy. Specimens shown in Figures 1, 2, 3, 16, 17, and 18 were among those studied by microprobe.

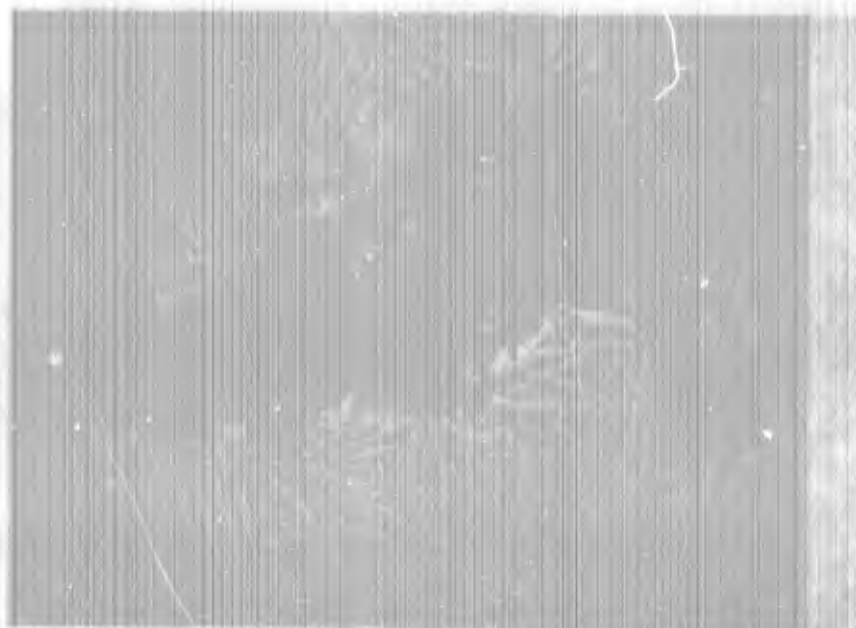


Figure 1. Defective region and alpha-stabilized reaction zone. Microprobe analysis of the small inclusions gave 6.9 to 8.8% N and less than 1% each of Al and V. Ti-6Al-4V. Originally 25X.

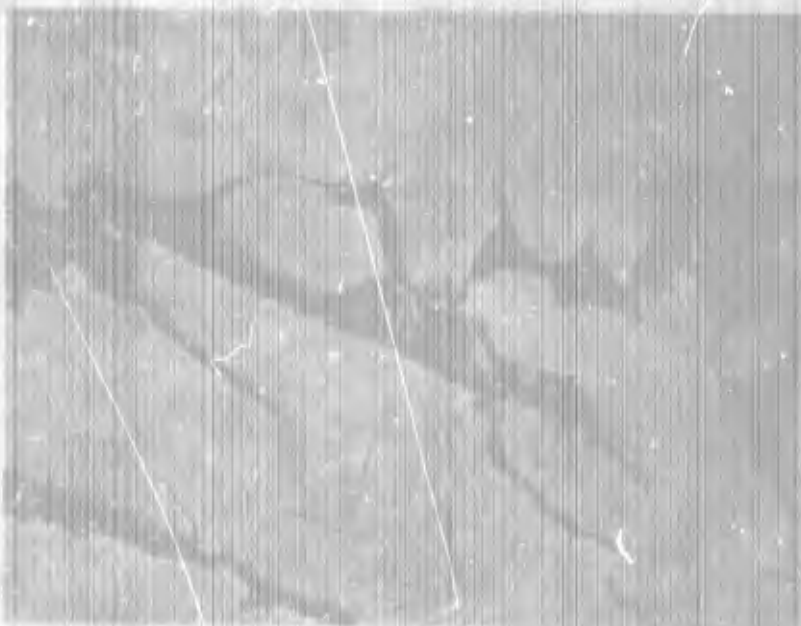


Figure 2. Magnified view of reaction zone in Fig. 1, showing two phases. Microprobe analysis gave 6.8% V and 4.5% Al in the dark phase, and 1.5% V and 6.0% Al in the light phase. Ti-6Al-4V. Originally 400X.

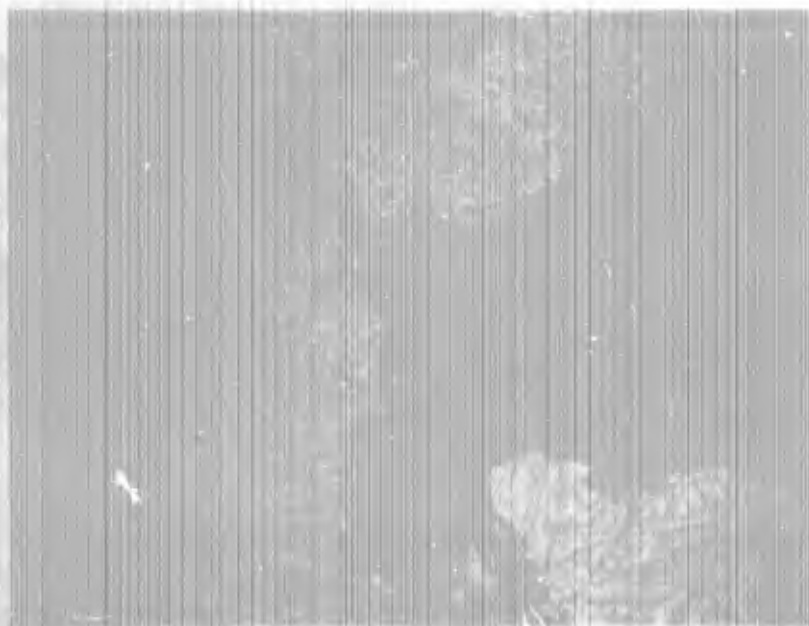


Figure 3. Defective region with inclusions and an alpha-stabilized zone.
Ti-6Al-4V. Originally 25K.

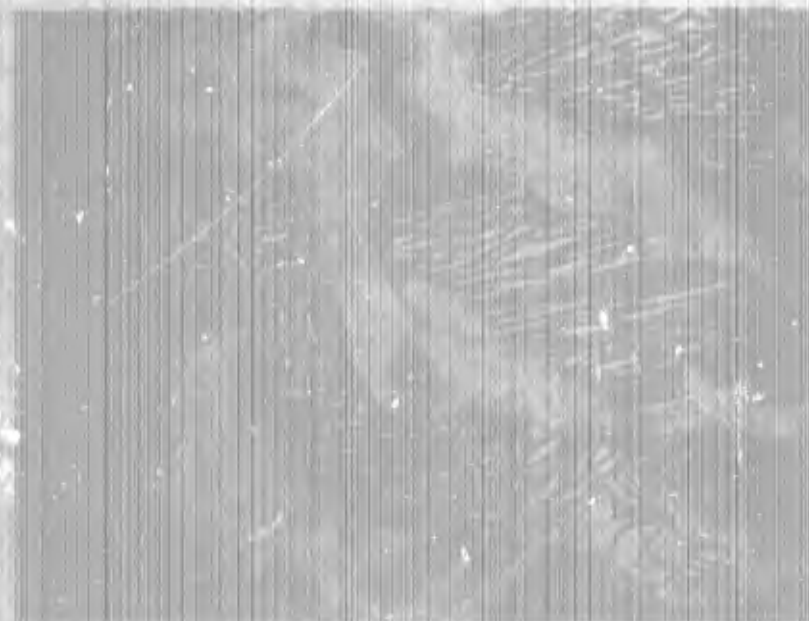


Figure 4. 300-degree structure of reaction zone in Fig. 3. Ti-6Al-4V.
Originally 400K.



Figure 5. Microstructure of the spongy inclusion in Fig. 3, probably 3 phases, predominately Ti_3Al (epsilon phase) according to X-ray diffraction. Ti-5Al-4V. Originally 400X.

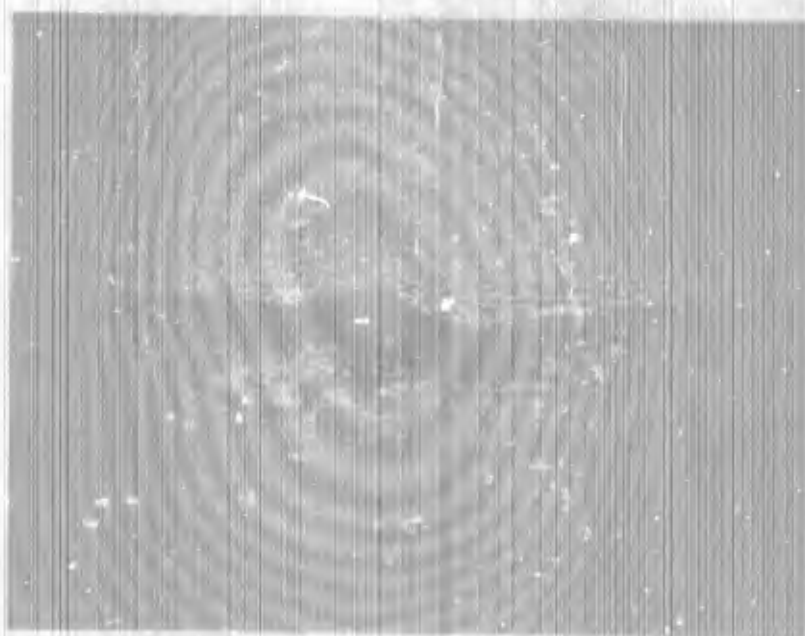


Figure 6. Elongated defect with a reaction zone. Ti-5Al-4V. Originally 25X.

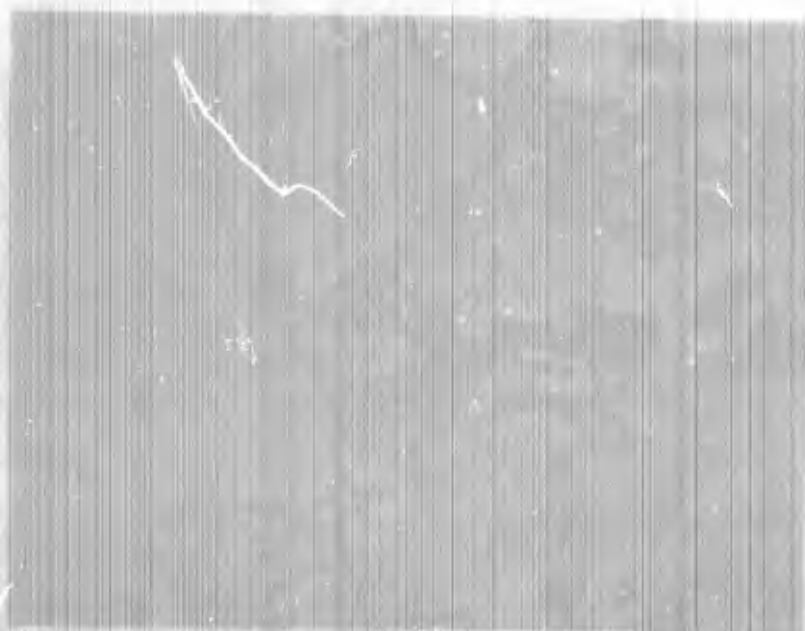


Figure 7. Two-phase reaction zones shown in Fig. 5. Ti-6Al-4V. Originally 400X.



Figure 8. Small alpha-coarsened defect. Ti-6Al-4V. Originally 30X.

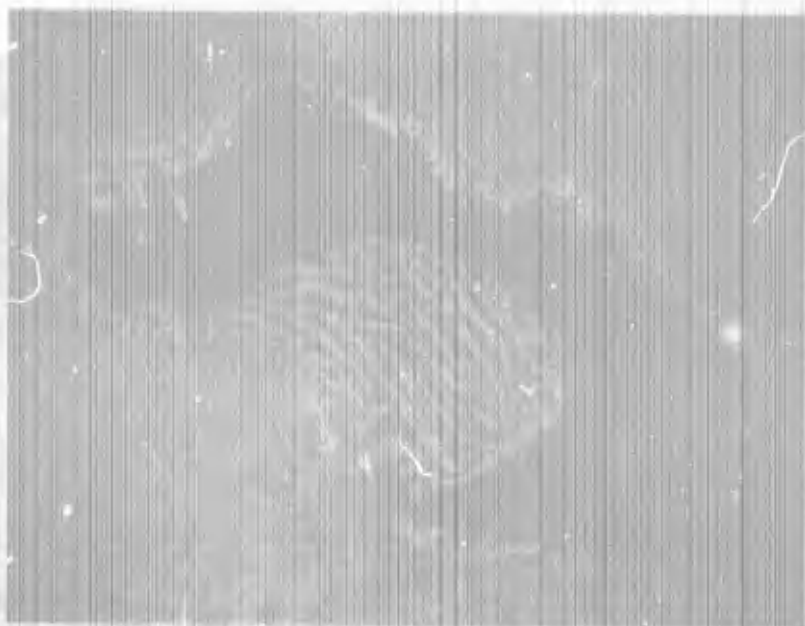


Figure 9. Defect with inclusions and reaction zone. Ti-6Al-4V. Originally 25X.



Figure 10. One of the spongy inclusions shown in Fig. 9. Microprobe analysis gave about 7.5% N. Ti-6Al-4V. Originally 600X.

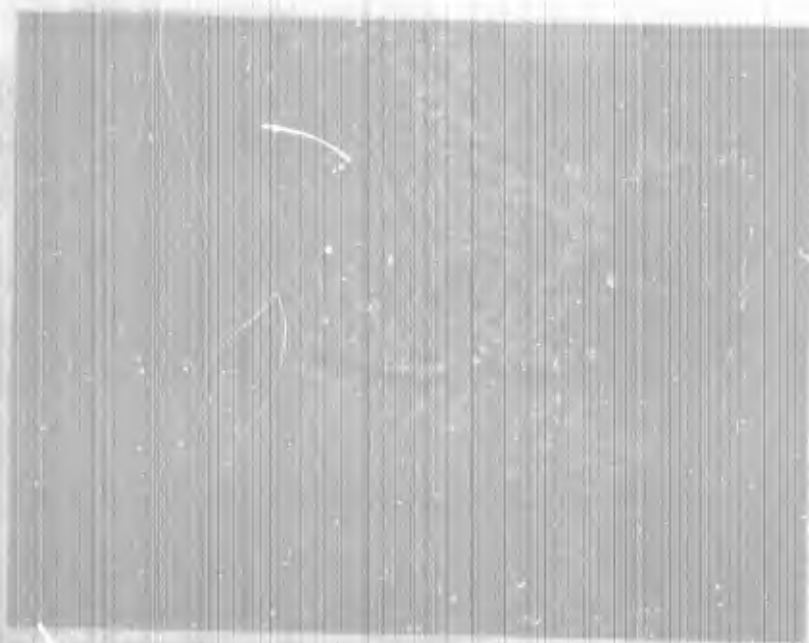


Figure 11. Defect with extensive alpha-stabilization and crack.
Ti-6Al-4V. Originally 85X.

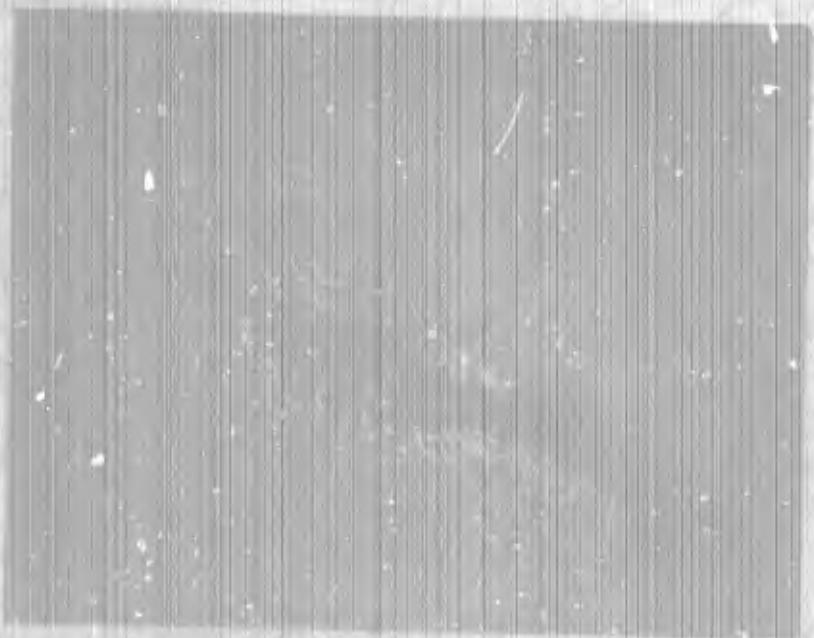


Figure 12. Elongated and cracked defective region. Ti-6Al-4V.
Originally 25X.



Figure 13. Defect with a limited reaction zone. Ti-6Al-4V.
Originally 20X.



Figure 14. Defective region with spongy inclusions. Ti-6Al-4V.
Originally 25X.

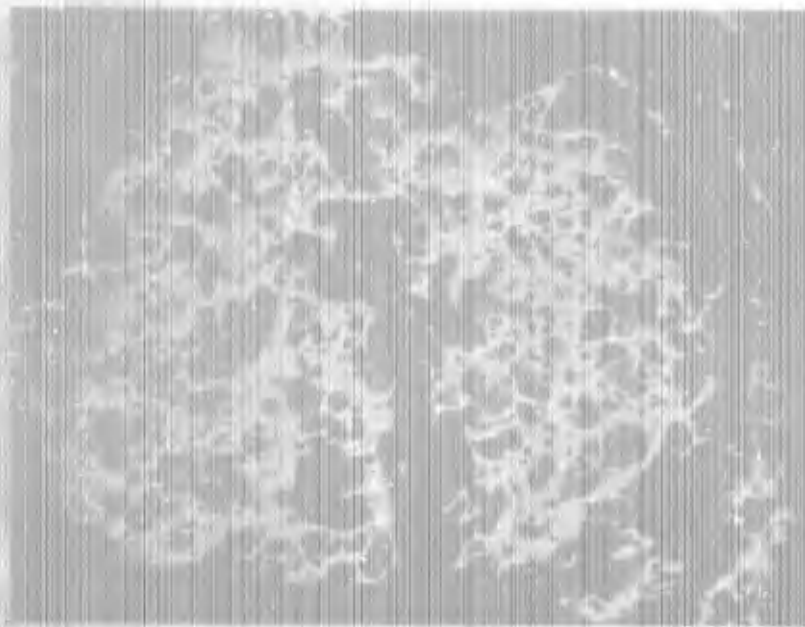


Figure 15. Spongy inclusion of Fig. 14. Ti-6Al-4V. Originally 400X.



Figure 16. Defect with unusually large inclusion fragment. Ti-6Al-4V. Originally 35X.



Figure 17. Defect and inclusions. Microprobe analysis gave about 5.7% Al and 2.1% Sn in the reaction zone. Ti-5Al-3.5Sn. Originally 500X.

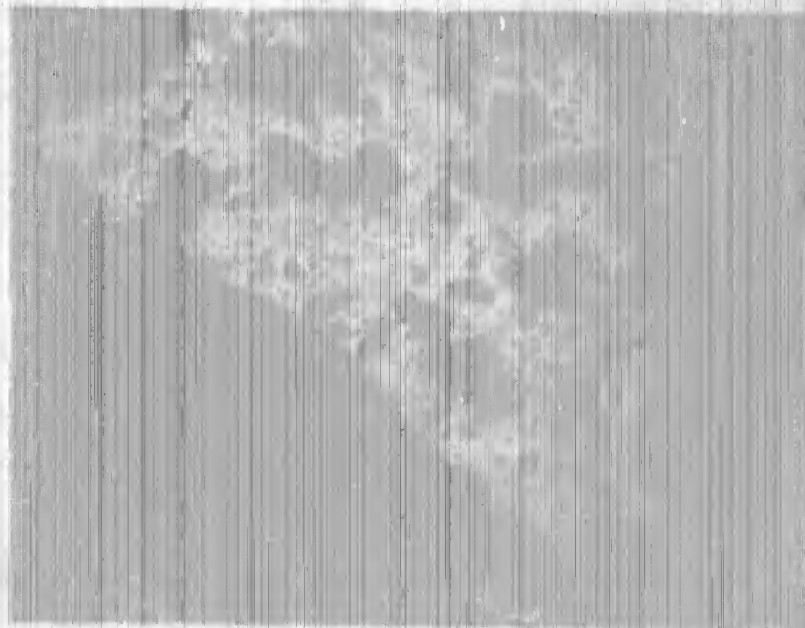


Figure 18. A spongy inclusion shown in Fig. 17. Microprobe analysis gave 11.9 to 14.8% N, 1.8 to 6.2% Sn, and less than 1% Al. Ti-5Al-3.5Sn. Originally 100X.

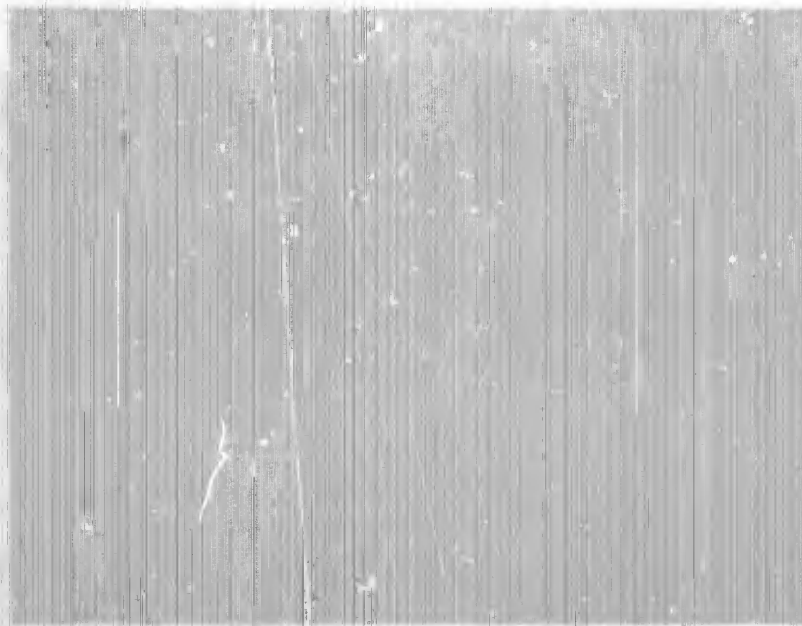


Figure 18. "Basket-weave" alpha-stabilized band, ultrasonically detectable.
Ti-5Al-2.5Sn. Originally 50X.

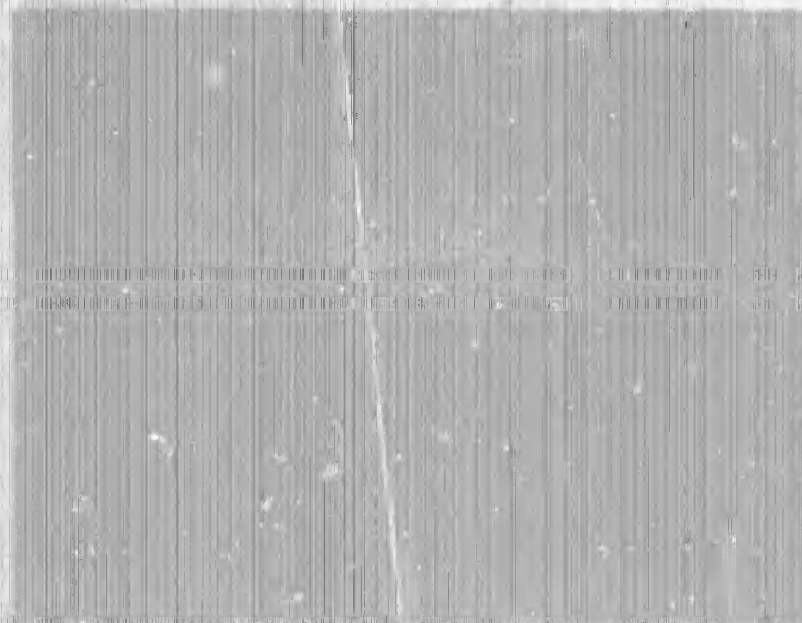


Figure 19. "Basket-weave" alpha-stabilized band, ultrasonically detectable.
Ti-4Al-4V. Originally 100X.

Inclusion fragments in thirteen of the fifteen doubly-melted specimens exhibited some degree of nitrogen enrichment ranging from 3.5% to 14.8%. Oxygen was definitely present in five cases at concentrations up to about 2.5%. In other cases, the oxygen was either absent or present in low concentrations. In a few specimens traces of carbon were detected too. It is not known how much of the oxygen and carbon might have been contributed by specimen mounting material or abrasives. Typically, alloy elements were heterogeneously segregated in the reaction zones around defects, but the nitrogen in the surrounding metal was below microprobe detection limits (about 1.5%). The two defects that were not of the nitrogen-rich type were a tantalum inclusion and a columbium inclusion.

Two of the defect specimens from first-melt metal were nitrogen-rich. One of these had an incoherent inclusion with 3.7 to 5.0% N. The other had an incoherent inclusion with 3.8 to 3.8% N, but aluminum enrichment up to 14.5% was also observed in those parts of the inclusion containing lower concentrations of nitrogen. The other two specimens had no concrete inclusions, but contained clusters of coarse alpha-phase grains in which the alloy content was low and there was some evidence of microsegregation. The nitrogen content was below detectable concentrations in these regions. The typical alloy analysis was about 3% Al and 1% V in one case, and about 2% Al and 0.5% V in the other. Incidentally, in all four specimens, severe grain-to-grain segregation of alloy was observed in the host structure away from defect sites. Most grains could be classed according to optical brightness or darkness. The bright grains were deficient in V (2.1, 2.2, 1.7, and 1.5%) and about normal in Al (5.9, 6.4, 6.5, and 4.8%). The dark grains were very rich in V (18.0, 17.5, 18.5, and 19.0%) and deficient in Al (2.5, 3.4, 2.5, and 1.6%).

2.3 Reduction-Process Experiments

To clarify the possible role of scavenging side reactions, as suggested in Section 2.1B, of this report, in causing refractory concentrations of nitrogen during titanium sponge production, nitrogen was deliberately introduced in various ways during a few experimental reductions of TiCl₄ by Mg. The reactor was a 6-inch-diameter, 36-inch-long vertical retort, with a lower-zone heater around the bottom 25 inches of the tube. Supported in the retort were a condenser shield, heat baffles, and a 4-inch-diameter by 10-inch high crucible with a sponge rack or "grid" 1-3/8 inches from the bottom. The retort, shield, and baffles were of austenitic stainless steel, and the crucible and rack were of ferritic stainless steel (type 430). After completion of a magnesium reduction, the crucible was inverted and supported over

the top of the retort, and by using an upper-zone heater the same retort served as a still for vaporization of salts from sponge. A typical charge for reduction comprised 900 ml of $TiCl_4$ and 500 grams of Mg which were reduced over 18 to 20 minutes at temperatures that were 800 to 850° C at the start and increased to about 875 to 900° C. The $TiCl_4$ was sprayed in continuously through an orifice under 5 psi pressure of argon. Vacuum distillation required 18 hours at 850° C.

The experiments are described in Tables III and IV. Magnesium was contaminated by melting it in the presence of various He- N_2 gas mixtures. In one case, the magnesium contamination was accomplished at the same time the $TiCl_4$ was reduced. In another case, the magnesium was given a preliminary nitrogen-contaminating treatment, but nitrogen gas was also present during the subsequent reduction. In both of these experiments, titanium sponge was contaminated directly as well as through the reductant. In the other two cases, $TiCl_4$ was reduced in the presence of pure He, so nitrogen in the Ti sponge should have come mainly from the pre-contaminated magnesium. Following each experiment, samples of the Ti sponge were obtained by splitting the crucible and its contents lengthwise and selecting regions of interest.

The experience is barely a beginning, but the trends are in expected directions. It is possible to introduce nitrogen contamination to titanium sponge indirectly through contamination of the magnesium used as a reductant. Not only is nitrogen transferred from the magnesium to the titanium, but it becomes concentrated near the bottom of the sponge mass in some of the first titanium formed during reduction.

TABLE III. - Conditions for Nitrogen Contamination of Magnesium Reductant

Experiment	Starting Partial pressures		Temperature	Time	N in Mg	Procedures/Uses
	He	N ₂				
4	100 torr	150 torr	800 to 900° C	20 to 30 minutes	Not sampled	He-N ₂ atmosphere maintained during TiCl ₄ reduction. Mg and Ti simultaneously contaminated.
5	440	66	700° C	10 hrs.	0.109%	Mg contaminated first, then TiCl ₄ reduced in pure He.
6	240	87	700° C	15 hrs.	Not sampled	Mg contaminated first, then TiCl ₄ reduced in residual He-N ₂ gas mix.
8	420	280	700° C	15 hrs.	0.075%	Mg contaminated first, then TiCl ₄ reduced in pure He.
9	400	360	800° C	15 hrs.	0.431% near top surface, 0.057% near bottom, and 0.575% in loose vapor-deposited powder.	Mg contamination run only. Not used for TiCl ₄ reduction.

TABLE IV. - Distribution of Nitrogen in Titanium Sponge Prepared With Contaminated Reductant and/or Reacting Gas

<u>Experiment</u>	<u>Sampled Region of As-distilled Sponge Mass ^{1/}</u>			
	<u>Upper outside</u>	<u>Center</u>	<u>Lower outside</u>	<u>Bottom</u>
4	228 ppm	366 ppm	351 ppm	0.13%
5	300	63	716	0.45%
6	1,370	3,230	5,280	1.64%
8	118	155	188	0.052%

^{1/} The open end of the crucible was taken as the top.

3. STUDY OF SYNTHETIC DEFECTS

3.1. Preparation of Nitrides and Oxynitrides

Because nitrogen-rich phases have a better chance of surviving in melting, because nitrogen frequently is a significant impurity in laboratory defects, and despite an apparent prevalence of oxygen contamination in sponge products, an emphasis on nitrogen-rich inclusions seemed most appropriate in experiments to observe the behavior of inclusions during melting. In these same experiments it was expedient to synthesize the defects to be studied rather than to rely on chance discoveries in commercial ingots. Therefore, the first step was the preparation of seed materials for artificially inducing defects in ingots.

Essentially stoichiometric TiN of at least 97% purity was obtained in two ways: either by purchasing powder from commercial suppliers, or by heating minus 35 mesh titanium sponge fines in flowing dry nitrogen for about 24 hours in a tube furnace at 1,000°C. The commercial methods of preparation are unknown, and there are several possibilities (18, 23, 24). The TiN was loosely pelletized, placed on a hearth of water-cooled copper, and fused by a tungsten-electrode arc in a He-Ar atmosphere (He used in one case) into buttons of about 35 to 40 grams each. About half of the nitrogen was lost in this process, although pressures of about 400 to 600 torr were maintained. The nitrogen analyses (Kjeldahl) of fused buttons are listed in Table V.

TABLE V. - Residual Nitrogen (wt. %) After Fusion of TiN

Button No.:	25,545 ^{1/}	25,924	25,935	26,163	26,185	26,186	26,187	26,171
Nitrogen:	13.4%	12.7%	11.1%	10.7%	12.4%	11.3%	10.3%	10.4%

^{1/} Nitrogen atmosphere used.

These buttons were broken to obtain fragments of various sizes for addition to ingots.

It was decided that, in addition to the binary Ti-N compositions, some ternary Ti-O-N materials would be especially interesting. Seeds for simulating defects, and information about formative conditions each were sought. Rather little has been published about the ternary system. The cation (Ti)-rich (1, 21) and anion (O,N)-rich (22, 27, 28) compositions have been given some attention, but no reports were found concerning intermediate materials. There is, however, enough information available on ternary phases with anion:cation ratios near unity to refute a flippantly repeated statement that TiO and TiN are completely miscible. There is definite evidence of intermediate phases in the system, and a limited solubility of TiO in TiN (23, 24, 28). The nitride does dissolve in the oxide up to about 40 mol % TiN, however. The system Zr-O-N also includes some intermediate phases and several of them that resulted from a solid-state reaction of ZrO₂ and ZrN have been studied (2), but the Zr-O and Ti-O binary systems are enough different that the respective oxynitrides are probably different too. Therefore, especially interesting phases to be expected in the ternary Ti-O-N system were prognosticated on the basis of binary Ti-O and Ti-N phases. The following points of relatively high stability summarize the nature of the binary systems:

- | | |
|---------------------|---|
| TiO | This phase has the NaCl structure and melts at about 1,360° C. The structure has numerous vacancy defects and a range of stoichiometry. |
| TiO _{0.80} | This is a peritectic composition with the NaCl structure at elevated temperatures. It is about the lowest oxygen content that still imparts the NaCl single-phase structure. The melting range is about 1,770° C to 1,780° C. |
| TiO _{0.70} | This is a hypo-peritectic composition with mixed NaCl and hcp phases for 925° C < T < 1,770° C. An intermediate phase (delta) with tetragonal structure is formed by peritectoid reaction at 925° C. (There may be some uncertainty about the T = 925° C value.) The melting range is about 1,770° C to 1,800° C. |
| TiO _{0.53} | This is a congruently-melting hcp solid solution with coincident liquidus and solidus maxima at about 1,800° C. |

TiN	This compound has the NaCl structure and melts at about 2,950° C. It dissolves Ti as a solid solution over a broad range of compositions.
TiN _{0.40}	This composition roughly corresponds to the low limit of nitrogen for retention of the NaCl single-phase structure. The melting range is about 2,500° C to 2,750° C.
TiN _{0.33}	This is a hyper-peritectic composition with mixed NaCl and hep phases for $T_x < T < 1,770^\circ \text{C}$ where T_x has been reported between 950° C and 1,593° C by various workers (24, 35). An intermediate phase (epitaxial) with tetragonal antirutile structure is formed by peritectoid reaction at T_x . The melting range is about 2,350° C to 2,950° C.
TiN _{0.26}	This is a peritectic composition with hep structure that melts from about 2,350° C to 2,600° C.

Consistency with the binary characteristics, and compatibility with normal thermodynamically based rules of phase diagrams are requisites that lead to an expectation that high-temperature phase equilibria for ternary combinations will resemble the hypothetical isothermal section shown in Figure 21, when someone gets around to a systematic study.

Experiments to prepare some of the oxynitride substances involved solid state reactions between TiO and TiN, mixed in a one-to-one molar ratio. First trials revealed that 900° C is an insufficient temperature, and that air must be completely excluded. Purging with commercial-grade inert gas is not enough protection to avoid oxidizing both TiO and TiN to rutile. In more successful experiments, mixtures have been encapsulated under vacuum in flame-sealed quartz tubes with inner liners of alumina tube, then heated to 1,250° C for 24 to 72 hours. Gas is liberated during an early stage of reaction, and somehow recombines later. Thus, the softened quartz envelope expands, then contracts. Several of the capsules have not survived such abuse, but four experiments have succeeded in producing single-phase materials with compositions near TiO_{0.6}N_{0.4} (see Figure 21). Results of chemical analyses and X-ray diffraction measurements are listed in Table VI. These materials were not available early enough in the overall investigation for extensive use as inclusion seeds.

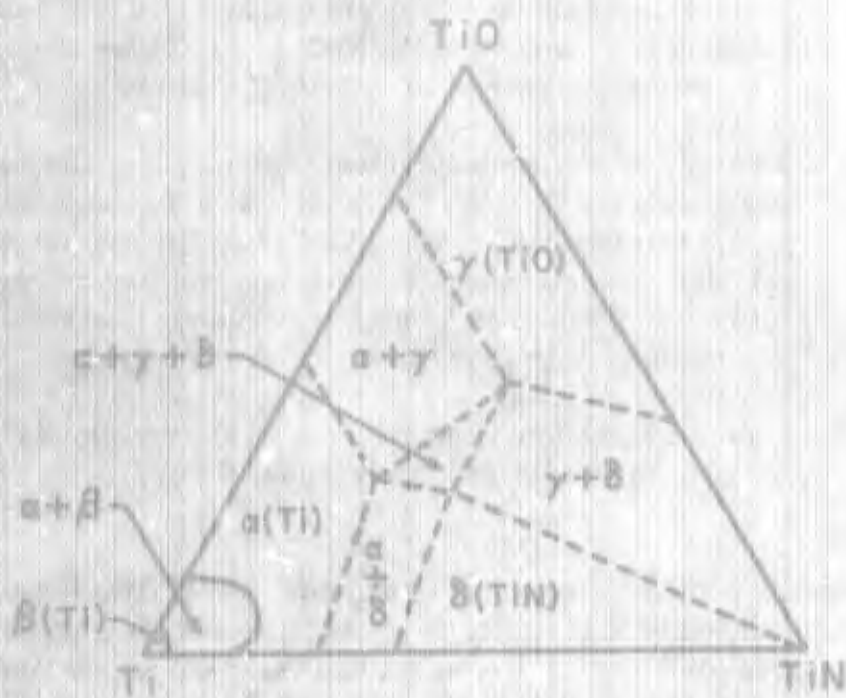


FIGURE 21 - Qualitative Suggestions for Phase Features of an Isothermal Section of about 1500° C, in the Ti-TiO-TiN System.

69-40

TABLE VI - Composition and Cubic Cell Size for Some Single-Phase TiO₂ N

Identification	By Chemical Analysis 1/		By Difference		Lattice Parameter, Å	Apparent Stoichiometry
	Ti	N	O	O		
T-3-3	72.1	11.5	14.6	16.4	4.208 ± 0.001	TiO _{0.68} N _{0.55}
T-3-3-1	73.6	10.8	13.4	15.6	4.214 ± 0.005	TiO _{0.63} N _{0.50}
T-3-3-2	75.3	9.5	12.5	14.2	4.2350 ± 0.0005	TiO _{0.56} N _{0.43}
T-4-2	75.0	10.1	13.5	14.9	4.226 ± 0.001	TiO _{0.59} N _{0.46}

1/ All analyses given in weight percent.

2/ Reliability of analysis for oxygen is questionable.

3.2 Magnesium-Titanium Sponges with Artificial Flaws

The feed material for most melting experiments was in the form of commercial electrodes. For first melting, the electrodes were cold pressed from sponge titanium with appropriate alloy and defect-seed additions. The sponges came from two commercial lots of magnesium-reduced, vacuum-distilled sponges. The vendor's analyses are listed in Table VII.

TABLE VII. - Vendor's Analyses of Ti Sponge ^{1/2}

Lot	C	O	N	H	K ₂ O	Cl	Al	Cu	Fe	Mg
A	50	150	10	-	-	-	50	<50	400	20
B	100	300	30	100	100	700	-	-	700	300

Lot	Mn	Ni	Si	Hardness rating
A	-	<30	150	120 Bhn
B	50	-	100	110 Bhn

^{1/2} ppm except as indicated.

The only alloy produced was Ti-6Al-4V. A master alloy of minus 8 mesh granules containing 34 w/o V and 13.6 w/o Al happened to be on hand, and it was combined with elemental aluminum for the alloy addition. The aluminum was obtained by cold rolling an unalloyed ingot to 1/4-inch plate and rolling it into small pieces. Principal impurities in the master alloy were 0.57% Fe, 0.70% Si, and 0.12% O. The aluminum was commercially pure with minimum purity of about 99%, and containing Fe, Si, and Cu as principal impurities.

Limited use was also made of some clean, chopped lathe chips from Ti-6Al-4V ingots that contained about 200 ppm C, 50 ppm H, 125 ppm N, and 340 hardness near 330 Bhn. This material was used in preparing a few small ingots (with Ti-defect-seeds added) by tungsten-electrode arc melting, and in quantities up to about 1/2 kg to protect the bottoms of copper melting crucibles from arc damage at the start of alloy ingot melts.

Sponge electrode bars were mechanically compacted in two nominal sizes — 1" x 1.5" x 10" and 2" x 3" x 10". The smaller ones were unalloyed, and the larger ones had the Al and V additions. The alloy was distributed as evenly as possible along the approximate center lines of bars. Seeds of fused nitride material usually were implanted at the center of each bar as shown in Tables VIII and IX.

The sponge compacts were welded into electrodes in helium, using thoriated tungsten welding electrodes in a totally enclosed, pre-evacuated, and sealed chamber. The electrodes were consumed into 3-inch to 5-inch-diameter crucibles or ladles of water-cooled copper by arc melting or electroslag melting in conventional shaft-type melting or casting furnaces. The basic equipment and procedures involved were recently reviewed elsewhere (5) and are not unusual. Some of the melting conditions, particularly pressure and arc current, will be specified in a later section of this report. Straight-polarity direct current (electrode negative) was used in all arc melts. Step-wise reduction and on-off cycling of power were employed at the ends of both arc and electroslag melts as a means of ingot hot topping.

In some experiments, magnetic stirring of the melt was used. This was done by means of a 1,000-turn solenoid of #20 magnet wire wrapped on the outside of a copper water jacket coaxial with a 5-inch-diameter crucible. Nominal dimensions of the coil were 8" diam. x 16" length, and it was operated at 2 amperes and 35 volts dc (2,000 ampere-turns) to provide a magnetic field directed upward approximately parallel to the longitudinal axis of the crucible (i. e. in the direction of applied voltage for straight-polarity arc melting). The result was a counterclockwise rotation of molten metal as viewed from above.

Another condition, imposed in two arc-melting experiments, was mechanical vibration of the molten pool during the melting operation. This too was done on the 5-inch-diameter scale. A heavy-duty pneumatic vibrator was bolted to the frame that supported the crucible and water jacket, and the entire assembly was shook. The frequency was surely not unique or constant, but the pitch was of a low acoustic magnitude, with dominant tones probably in the range of 50 to 200 cps as estimated by comparison with tuning forks. In any case, the effect in operation was to cause standing nodas on the molten metal surface at peak-to-peak spacings in the order of a centimeter.

TABLE VIII. - Defect Seeding of Unalloyed Electrode Bars

Bar number	Seed description ^{1/}	Seed weight	Bar use (Ingot number)
1	1 pc. of SA 25,926	2,000.0 mg	SA 25,936
1a	do.	1,806.0	SA 25,947
2	do.	866.0	SA 25,936
2a	do.	811.2	SA 25,947
3	do.	524.1	SA 25,936
3a	do.	510.0	SA 25,947
4	1 pc. of SA 25,924	1,770.0	SA 25,937
4a	do.	1,747.1	SA 25,948
5	1 pc. of SA 25,926	872.4	SA 25,937
5a	do.	862.9	SA 25,948
6	1 pc. of SA 25,924	597.1	SA 25,937
6a	do.	636.3	SA 25,948
7	do.	1,374.7	SA 25,939
8	1 pc. of SA 25,926	849.5	Do.
9	do.	646.1	Do.
10	do.	1,311.0	SA 25,940
11	1 pc. of SA 25,924	1,166.5	Do.
12	1 pc. of SA 25,926	679.7	Do.
13	do.	1,262.6	SA 25,941
14	1 pc. of SA 25,924	1,035.7	Do.
15	1 pc. of SA 25,926	745.5	Do.
16	1 pc. of SA 25,924	1,271.1	SA 25,942
17	do.	1,057.5	Do.
18	do.	781.1	Do.
19	do.	1,232.9	SA 25,944
20	do.	1,071.1	Do.
21	1 pc. of SA 25,926	785.5	Do.
22	1 pc. of SA 25,924	1,200.5	SA 25,945
23	1 pc. of SA 25,926	838.3	Do.
24	1 pc. of SA 25,924	983.2	Do.
D/2-1	1 pc. of SA 25,924 ^{2/}	1,870.0	SA 25,561
	do.	1,582.7	Do.
	do.	1,241.0	Do.
D/2-2	do.	351.1	Do.
	do.	819.8	Do.
	do.	614.7	Do.
D/2-3	do.	380.4	Do.
	do.	342.5	Do.
	do.	192.5	Do.

^{1/} Refer to Table V.

^{2/} Three pieces spaced 3" apart in bars instead of 1 piece at center.

TABLE IX. - Defect Sizing of Ti-6Al-4V Electrode Bars

Bar number	Seed description ^{1/}	Seed weight	Bar size (inset no.)
1	1 pc. of SA 25, 928	568.5 mg	SA 26, 194
2	bits and fines of SA 25, 924	995.6	Do.
3	bits and fines of SA 25, 545	608.4	Do.
4	6 pcs. of SA 25, 545	717.6	SA 26, 207
5	1 pc. of SA 25, 926	690.3	Part ruined, part to SA 26, 237
6	3 pcs. of SA 25, 545	900.0	Ruined
7	fines of SA 25, 924	471.2	SA 26, 209
8	1 pc. of SA 25, 926	1,440.0	Do.
9	1 pc. of SA 25, 926	530.6	Do.
10	bits and fines of SA 25, 545	734.2	SA 26, 206
11	bits and fines of SA 25, 545	893.0	Do.
12	2 pcs., bits, and fines of SA 25, 928	977.6	Do.
13	1 pc. of SA 25, 928	1,147.0	SA 26, 606
14	bits and fines of SA 25, 545	711.8	Do.
15	4 pcs. of SA 25, 545	805.6	Do.
16	1 pc. of SA 25, 926	1,440.9	SA 26, 195
17	bits and fines of SA 25, 545	528.4	Do.
18	3 pcs. of SA 25, 545	704.4	Do.
19	1 pc. of SA 25, 926	830.9	SA 26, 207
20	bits and fines of SA 25, 926	772.6	Part ruined, part to SA 26, 207
21	6 pcs. of SA 25, 926	835.2	Ruined
22	bits and fines of SA 25, 545	1,005.8	SA 26, 212
23	bits and fines of SA 25, 545	592.5	Do.
24	6 pcs. of SA 25, 545	868.0	Do.
25	1 pc. of SA 25, 926	1,160.9	SA 26, 214
26	18 bits of SA 25, 924	660.2	Do.
27	7 pcs. of SA 25, 545	504.8	Do.
28	5 pcs. of SA 25, 545	677.2	SA 26, 230
29	10 bits of SA 25, 924	564.2	Do.
30	1 pc. of SA 25, 926	1,468.1	Do.

^{1/} Refer to Table V.

When ingots were prepared by skull casting instead of the more conventional gradual solidification method, they were poured under unassisted gravitational force into 4-inch cylindrical molds of commercial graphite that had a bulk density near 1.7 g/cc and that typically leaves less than 0.2% residue after melting. The nominal diameter of the casting ladle and residual skull was 3 inches.

In electrolytic melting, purified water-free calcium fluoride was the slag. Straight-polarity direct current was used for heating in a straight-forward manner (2).

Most of the ingots produced were first split lengthwise. Then the exposed interior faces were roughly flattened, as with a lathe or grinding machine, and given a coarse polish with silicon carbide abrasive. The polishing was done on either a 24- or a 36-inch lapping table, as appropriate for the size of the particular ingot half. Water, both with and without a liquid detergent, was used as a vehicle for 240-grit abrasive on a reinforced rubber backing and 600-grit abrasive on felt. The work piece was placed flat down on the polishing surface inside a retaining ring with a diameter slightly larger than the maximum dimension of the work piece. As the polishing wheel turned, the retaining ring was free to roll against a larger fixed ring that formed a sector near the outside edge of the circular table. Thus, the ingot half was forced to slip on the polishing wheel and rotate about the approximate center of the retaining ring. With the help of some artistry and experience concerning such things as consistency of the abrasive mixture, the procedure usually was adequate to delineate defects in the ingot sections. It was also tedious and time consuming.

Ingot sections were examined as-polished and after etching with a 6:4 solution of concentrated nitric and hydrofluoric acids. The overall defectiveness was evaluated and selected areas of special interest were cut out, mounted in plastic, and given a more careful metallographic treatment. The special mounts were polished with various combinations of diamond in oil and alumina in water down to 0.05 micron in fineness, on a variety of polishing surfaces. Both optical and electron-microprobe metallography were used on both as-polished and lightly etched specimens. The etchant was an aqueous dilution, typically by half, of the same acid combination used for the heavier etching.

Most of the once-melted ingots were eventually remelted. Depending on dimensional restrictions in the remelt electrode, some ingot sections were reduced to quarters by another longitudinal cut. Halves or quarters, as necessary, were welded together into remelt electrodes using the same

welding chamber used for fabrication of the first melt is detailed. Metals not remelted included several specimen sections, a few ingots that were rejected because of spurious contamination and other processing irregularities, an ingot half that was extensively sectioned in an examination approaching total destruction, and four 2-inch ingots that were rolled to plate to test the response of defects to deformation.

Rather surprisingly, attempts to synthesize defects were not too successful in buttons are melted with a horizontal tungsten electrode. The main problem was a lack of confidence in our ability to expeditiously locate any and all flaws that may have survived. Typically, a single defect seed per button was desired, and there was little consistency in the locations where remnants of these were found, or in the apparent chance of finding any remnant. There was a nagging suspicion that seeds were being disassociated or otherwise lost without ever really getting into the molten pool. Belatedly, a procedure was adopted wherein about 40 grams of the machine chips previously described were melted into a button. Then a small-bore well was drilled into the bottom side of the button. The defect seed was placed in the well, and the button was remelted, well side up. In the limited use that was made of this technique, it appeared that the well rims quickly melted in to cover the seed and prevent its spurious loss, and that seed remnants could be found near the site of the well bottom.

3.3 Nature and Behavior of Nitride Defects

The seeds used for causing artificial defects were more than ample. Most ingots contained numerous flaws due to the nitrogen-rich additions. Thus, the single evaluation cut used for most ingots provided an adequate, but not infallible, index of relative defectiveness. Overall, the experience with synthetic defects confirmed the observation with defective commercial ingots that the alpha-stabilized flaws are apt to be in the lower parts of ingots. In addition, there was a tendency for synthetic defects to favor centerline positions in ingots. These two traits enhanced the validity of the single-cut estimate of defectiveness, and each is consistent with a mechanism of defect survival by sinking to the pool bottom.

Two other general observations were a tendency for fused nitride lumps to become fragmented in arc melts, and a frequent discovery of pinhole per sity and/or micro-porosity near defect sites. In arc melts, and particularly those at low pressure, the sizes of refractory lumps that survived were smaller than the sizes of the input seeds. This was not true in

electroslag melting. In fact, the lumps seemed to survive electroslag melting quite intact with little alteration. Accordingly, the fragmentation during arc melting is presumed to be a consequence of some action of the arc itself. Indeed, the observation seems to be consistent with a prevalence at low pressures of a mode of arc operation that has been described as "skittering arc" (2), although it is also consistent with the existence of deeper molten zones in arc melting.

Three types of synthetic defects were recognized. They are illustrated in Figures 28 through 30. Type I defects are incoherent inclusions of one or more brittle phases surrounded by a hard alpha-stabilized reaction zone. Type II defects are coherent inclusions of microscopically separated, easy, alpha-stabilized phases. They resemble the coarse-structured reaction zones associated with type I defects, but without the incoherent inclusion. Because of their hardness they tend to stand out in relief on a polished surface. Type III defects also are coherent, but phases are separated on a microscopic scale that makes it difficult to characterize minor phases. Properties to the micro-inclusions, lattice expansion, hardening, and corrosion susceptibility are noticeable in the host structure. The last property mentioned, corrosion, is the key to locating the type III defects by microscopic inspection. An HF-HNO₃ etchant preferentially pits the type III regions and makes them appear bright with normally reflected light, or dark with obliquely reflected light. This behavior is shown in Figure 30. Figure 30 also exhibits a tendency of type III defects to be clustered in some of the late-freezing and slowly-cooling metal at the core of an ingot. In an unaligned remelt ingot (not shown), five clustered type III defects had Knoop microhardnesses (2 kg load) of 396.2, 301.2, 214.8, 194.0, and 177.6. Two apparently normal grains nearby had microhardnesses of 114.8 and 116.1.

Quantitative microprobe analysis, using nitrogen K-alpha X-ray emission in conjunction with micrography indicates that the incoherently included parts of type I defects probably contain three phases. Results corresponding to Figures 23, 24, and 25 are given in Table X.

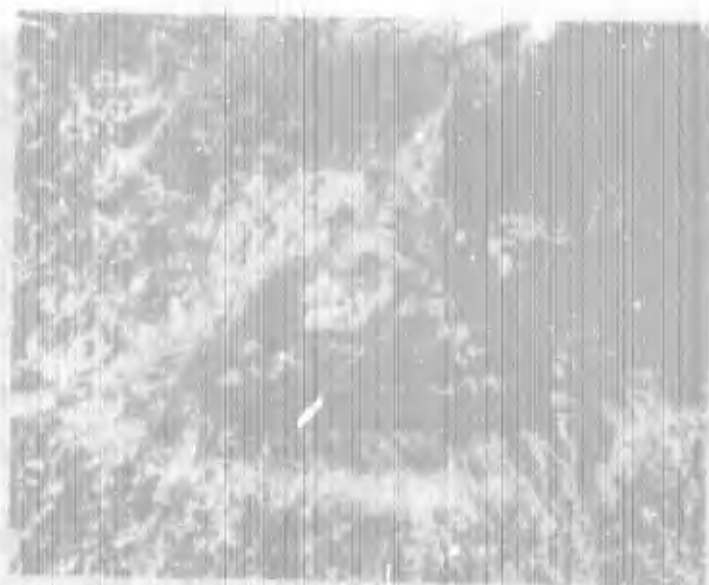


Figure 22. Specimen 897U. 3 second view, oblique light. Detail at tip of type I defect. Originally 35X.



Figure 23. Specimen 897L. Microprobe back-scattered electron image. Type I defect and basket-weave reaction zone. Originally 150X.

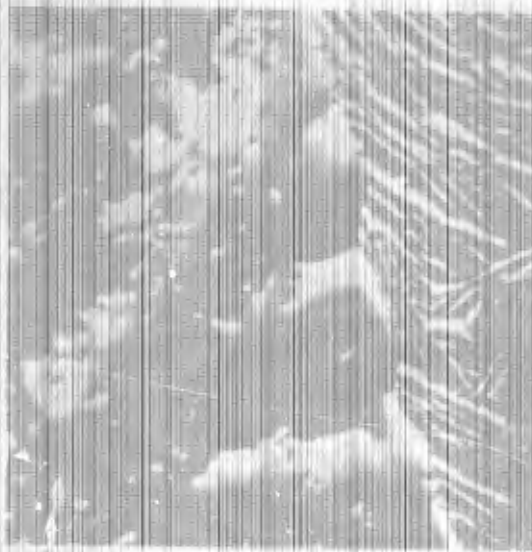


Figure 24. Specimen 937U. Microprobe back-scattered electron image.
Type I defect and basket-weave reaction zone.
Originally 150X.

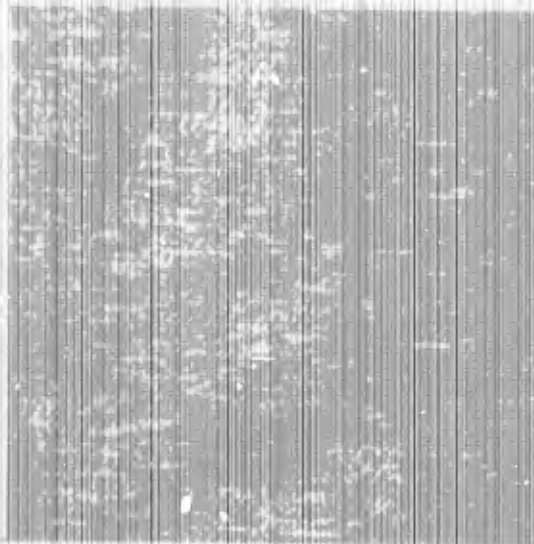


Figure 25. Specimen 937U. Microprobe X-ray pattern of nitrogen,
corresponding to Fig. 24. Originally 150X.

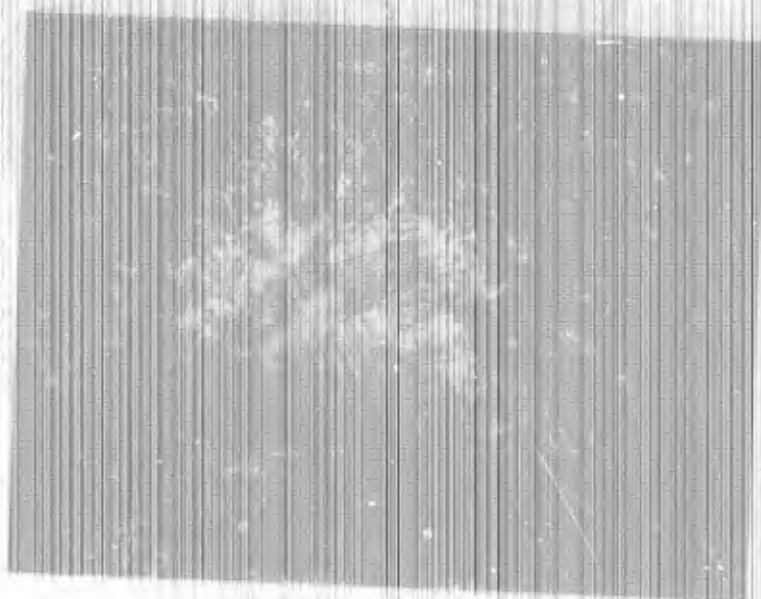


Figure 26. - Specimen 937U. 3 sec. etch, oblique light. Detail of type II defect. Originally 25K.

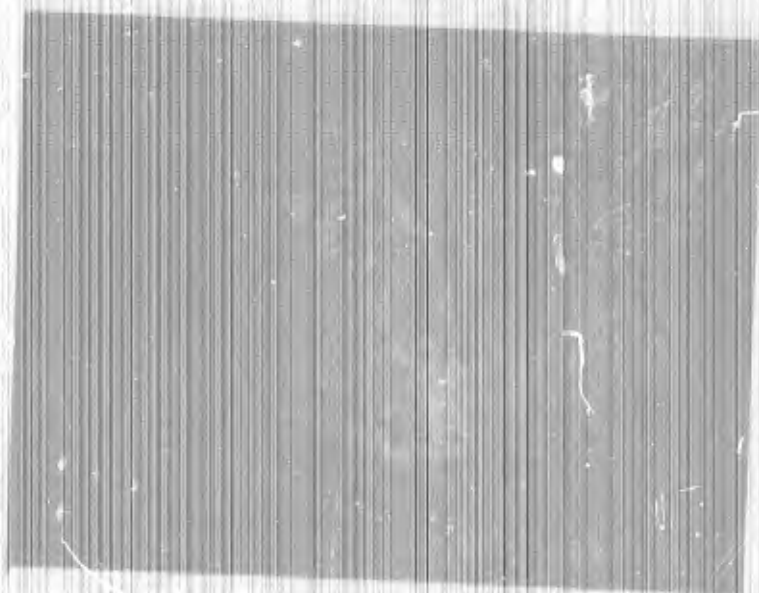


Figure 27. Specimen 951B. 3 sec. etch, oblique light. Type III defective region. Originally 25 K.

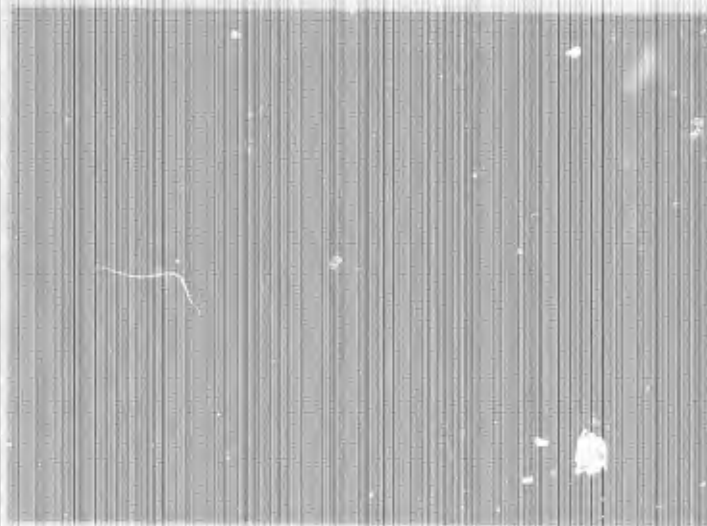


Figure 28. Specimen 951B. 3 sec. etch, oblique light. Another type III defective region. Originally 25K.

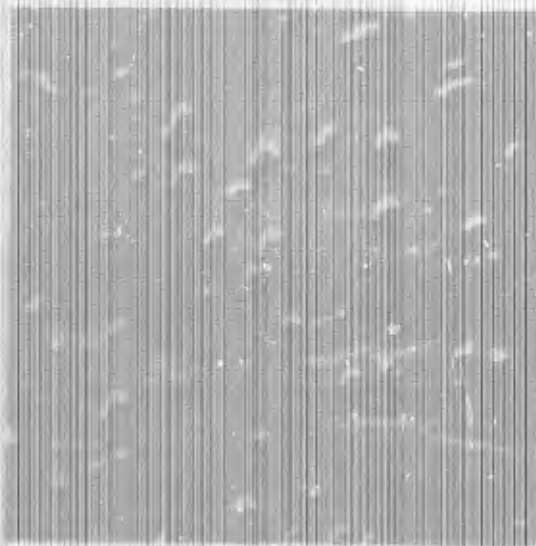


Figure 29. Specimen 951B. Microprobe back-scattered electron image of type III defect. Originally 250K.

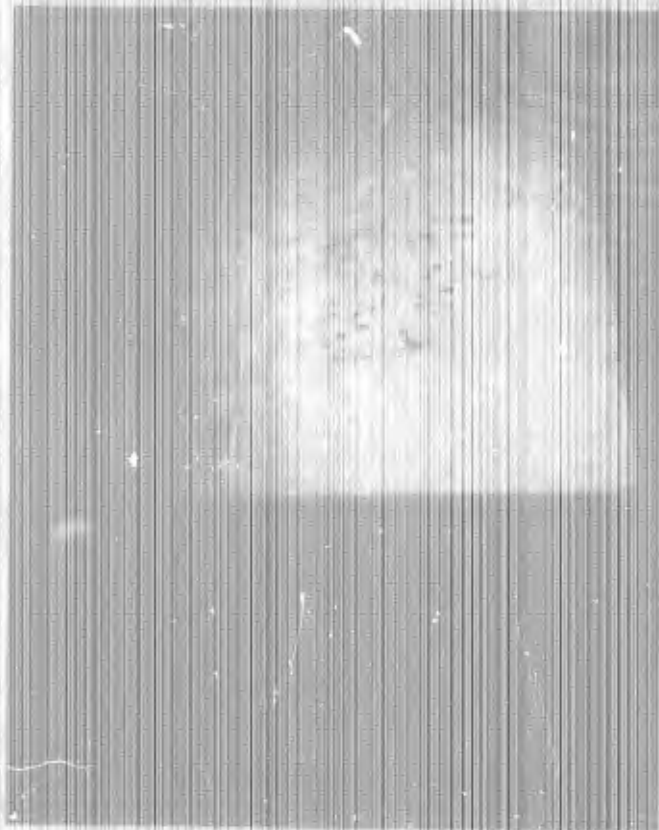


Figure 30. Etched ingot section showing appearance of type III defective regions.

TABLE X. - Nitrogen Distribution in Type I Defects

<u>Specimen</u>	<u>Region</u>	<u>w/o N</u>
937 L	Frothy patches	11.3 ± 0.5
937 U	do.	15.5 ± 1.5
937 L	Smooth spots, interior only	7.2 ± 0.5
937 U	do.	8.9 ± 1.0
937 L	Smooth rim at inclusion edge	4.8 ± 0.5
937 U	do.	2.8 ± 0.5
937 L	20 micron outside inclusion	< 1.5
937 U	do.	< 1.5

Three separate levels of nitrogen contamination are evident. Although structures are not revealed by the sort of analysis used, the compositions, in the order of decreasing nitrogen, correspond roughly to a delta-phase solid solution of Ti in TiN with a fcc rock-salt structure, the epsilon intermediate phase of approximate stoichiometry Ti_2N with a tetragonal structure, and an alpha-phase (hcp) solid solution of N in Ti, respectively.

The nitrogen content of the type II defects seems to be similar to that of the reaction zone around type I defects. Both are below detection limits for microprobe analysis. The micro-inclusions in the type III regions are too small to yield quantitatively readable X-ray intensities, but the emission qualitatively reveals that the "average" atomic number of the inclusions is lower than the surrounding metal. Incidentally, although it is not always easy to tell in a photographic reproduction, the "spots" in Figure 26 project out from the specimen, and they are inclusions. Also, a few of the pits in Figures 27 and 28 may be porosity, but most of them are sites where inclusions were pulled out during polishing.

The radiographic response of some of the synthetic defects was studied briefly. The main intent was to test the chance of finding artificial flaws in buttons. Some germane radiographic parameters are listed in Table XI.

TABLE XI - Some Radiographic Parameters for 0.3 Angstrom X-rays

Substance	Specific Gravity, g/cc	Mass Absorption Coefficient, sq cm/g	Linear Absorption Coefficient, cm ⁻¹
10 w/o N in Ti	4.84 ^{1/}	1.92 ^{1/}	9.8
9.5 w/o N and 14.2 w/o O in Ti	5.08 ^{1/}	1.64 ^{1/}	8.4
4 w/o O in Ti	4.56 ^{1/}	2.33 ^{1/}	9.2
Ti	4.52	2.1	9.45
Ti-6Al-4V	4.43	2.02 ^{1/}	8.95

^{1/} Calculated by conventional methods of weighted averaging.

The first three tabulated compositions correspond to the seeds added to buttons. The most successful tests involved 120 kv X-rays from a tungsten target bombarded by five milliamperes of electron current. Type M film was used at a distance of 3 feet with lead backing and a front screen of 0.32-mil aluminum foil. Exposure times were between 5 and 10 minutes for subject thicknesses of about 5/16 inch to 1/2 inch. Film was developed in Kodak X-ray developer 5 minutes and fixed 10 minutes, both at 68° F, with appropriate rinsing and washing.

Because of questionable success in retaining seeds in earlier button melts, very conservative conditions, including only 200 amperes of current, were used in melting buttons as radiographic specimens. Both the nitrided material (10% N) and the oxynitride caused inclusions that were radiographically observable in Ti-6Al-4V buttons. The oxygen-rich material apparently left only a small gas hole. There was also some indication of sponginess or porosity associated with the inclusions due to the nitride and oxynitride. Ratios of radiographic film densities resulting from a 5-minute exposure were $D_x/D_o = 1.03$ for the nitrided seed and $D_x/D_o = 1.15$ for the oxynitride seed, where D_x corresponds to the minimum intensity transmitted through the Ti-6Al-4V button adjacent to the inclusion. Thus, inclusions due to either

nitrides or oxynitrides would seem to be somewhat more transparent to X-rays than the matrix alloy. However, this result probably was influenced by the presence of porosity. Ideally, according to Table XI, the nitride-caused inclusion should have been slightly less transparent, but the disagreement is not great.

Another object radiographed was a 1/2-inch-thick slice from the bottom of an unalloyed 3-inch ingot (No. SA 28,940) of nitride-seeded titanium. The slice was known to contain several type I and II defects of about 5 to 10 mil size that were exposed at the surface by polishing. The same conditions were used for radiography of this piece except that best results were obtained at exposure times near 10 minutes. Shadows of the small inclusions were barely discernable, but only because locations of some of them were already known from inspection of the subject. These inclusions were slightly less transparent to X-rays than their unalloyed host metal. Again, this is contrary to expectation, based on ideality (see Table XI).

The thermal stability of type I defects was checked in a very cursory manner by an annealing test for 3 hours at 1,100° C in vacuum. An unalloyed specimen (from SA 26,285) with a type I defect, about 3 mm across, exposed at the surface, was heat treated. There was no substantial change in the bulk of the inclusion, nor any healing of the interface between the inclusion and the matrix. However, for a distance of about 0.2 mm beyond the edge of the inclusion, the surface of the matrix structure acquired a stained appearance. There was no noticeable change in grain structure near the inclusion. The stain may have been caused by surface diffusion or by chemical action of decomposition products from the inclusion.

In one sense, another test of thermal stability was included in some rolling trials. However, the main purpose of the work was simply to test the responses of defects to deformation. Halves of four unalloyed, 3-inch ingots were hot rolled from about 1-5/16-inch thickness to about 1/2 inch. A nominal reduction in thickness of 10 percent was achieved in each of several passes — 40 percent overall. One half of each ingot was rolled at 850° C (normally alpha condition) and the other half was rolled at 1,000° C (normally beta condition). Initial heating was for 30 minutes, then each piece was reheated 5 minutes between passes. After rolling, each plate was reheated again, flattened in a forging press, air cooled, and sand blasted.

The face of each plate, corresponding to the interior longitudinal cross section that was previously annealed for defects, was coarsely polished and re-annealed in as-polished and etched condition. Typical observations are illustrated in Figures 31 through 37. In general, the brittle parts of type I defects crumbled and were lost, as shown in Figures 31 and 35. Only when they were quite small, were type I defects retained reasonably intact, as shown in Figure 33. The type II defects tended to remain as hard, coherent inclusions (see Figures 33 and 35). Under the experimental conditions, type II defects did not initiate cracks or tears, but they seemed to resist deformation and it is likely that they would cause more trouble in thinner plate or sheet. They might also behave poorly if fatigued. As expected, the type III defects were least troublesome, as shown in Figures 34 and 35. More careful preparation of the surface shown in Figure 34 may reveal that the striations that can already be seen represent deformation twins. If so, it probably means that the type III region remained in the hex phase condition at 1,000° C. Cubic body-centered structures can deform by twinning, but they rarely do, and usually on a much finer scale.

Figure 37 illustrates an unusual behavior of type II defects that must be considered an anomaly. It occurred in only one plate, but as three scattered sites on the surface of that plate. It appears that the hard defect core was extruded out of the surface, leaving a hole behind and forming a lump nearby where it was pressed into the surface by the rolls. Except for this particular anomaly, the behavior of type II and III defects seemed to be slightly less objectionable when rolled at the lower temperature.

Within the available time, rolling tests and examinations of deformed films have been very cursory. The results should be received accordingly. More extensive and more careful study of this aspect of behavior is warranted.

Despite some doubts because of brevity and shallowness of the investigation, a rather consistent pattern of behavior has been sketched for the nitride-induced defects. Thus it seems appropriate to close this description of behavior with some conjecture about underlying reasons. In this connection, the phase diagram presented in Figure 38 is useful.

The close correspondence between the nitrogen contents of defect nuclei and the bulk of type I inclusions makes it clear that the type I defects are essentially unreacted fused nitride (compare Tables V and IX). Their locations in ingots indicate that they avoid melting by sinking to the bottom of the pool where the temperature is near the melting point of titanium and, for most

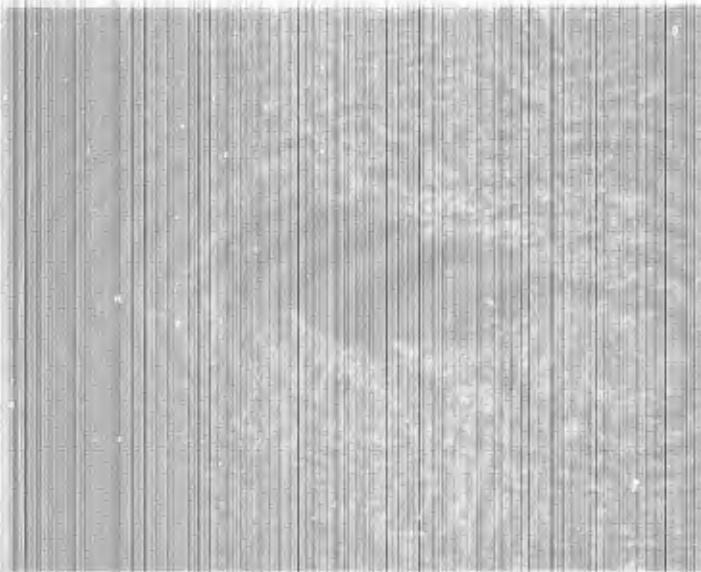


Figure 31. Type I defect in unalloyed plate 945B after rolling at 1,000° C. Polished with 600 grit SiC, HF-HNO₃ etch. Originally 25X.

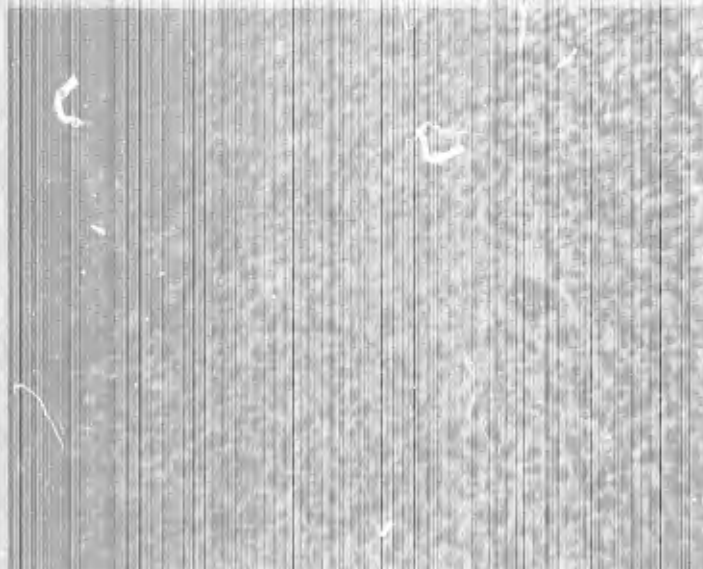


Figure 32. Two small type I defects in unalloyed plate 945B after rolling at 1,000° C. Polished with 600 grit SiC, HF-HNO₃ etch. Originally 12X.

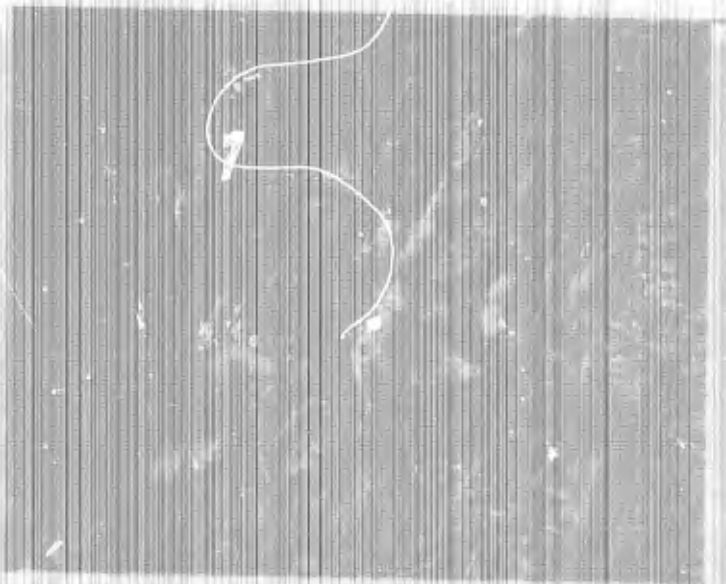


Figure 33. Type II defect in unalloyed plate 948B after rolling at 1,000° C. Polished with 600 grit SiC, HF-HNO₃ etch. Originally 25X.

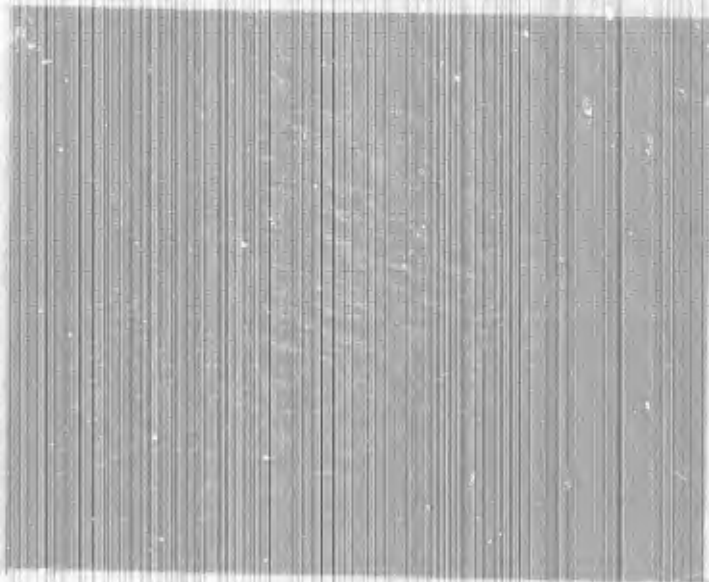


Figure 34. Type III defect in unalloyed plate 948B after rolling at 1,000° C. Polished with 600 grit SiC. Not etched. Originally 12X.

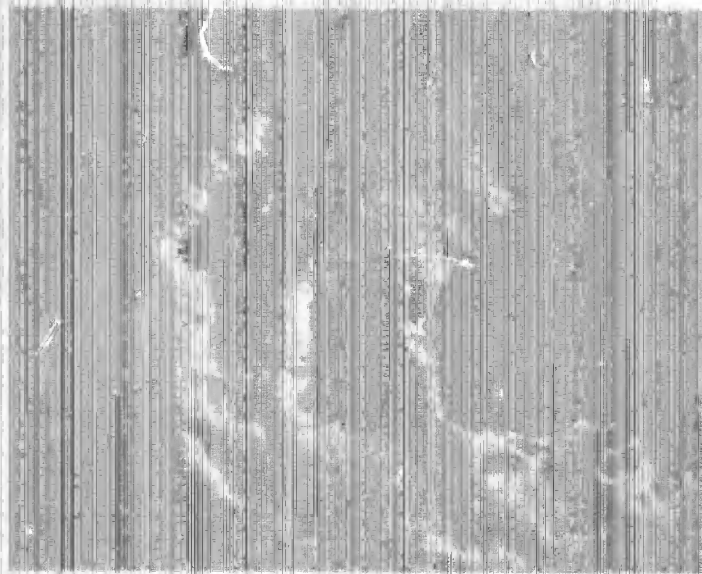


Figure 35. Type I defect in unalloyed plate 947A after rolling at 850° C. Polished with 240 grit SiC. Not etched. Originally 12X.

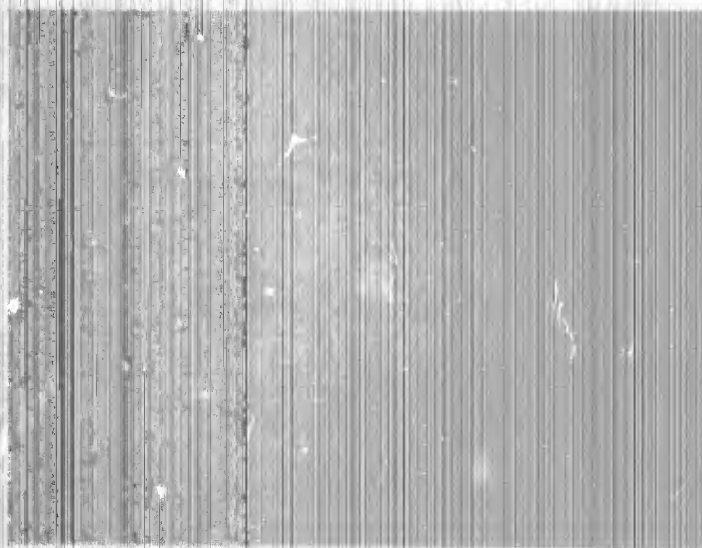


Figure 36. Type II (bright) and type III (dark) defects in unalloyed plate 946A after rolling at 850° C. Polished with 240 grit SiC. HF-HNO₃ etch. Originally 6X.

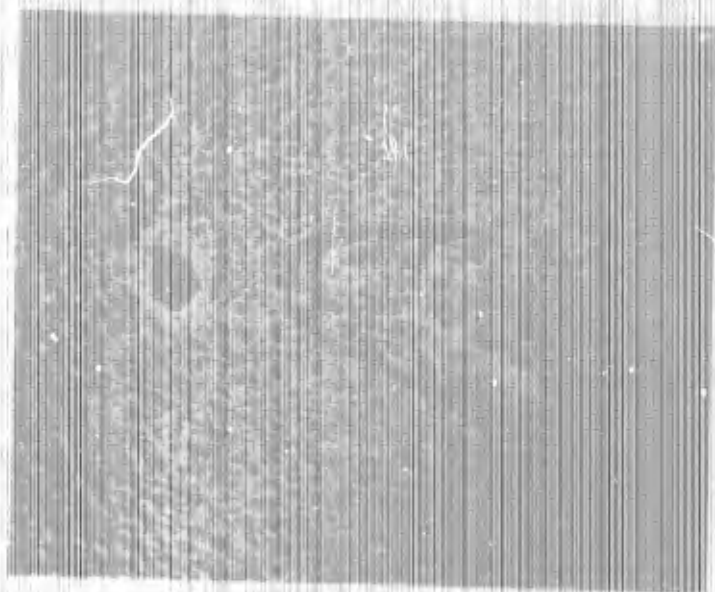


Figure 37. Anomalous type II defect in unalloyed plate 940A after rolling at 850° C. Polished with 600 grit SiC. Not etched. Originally 12X.

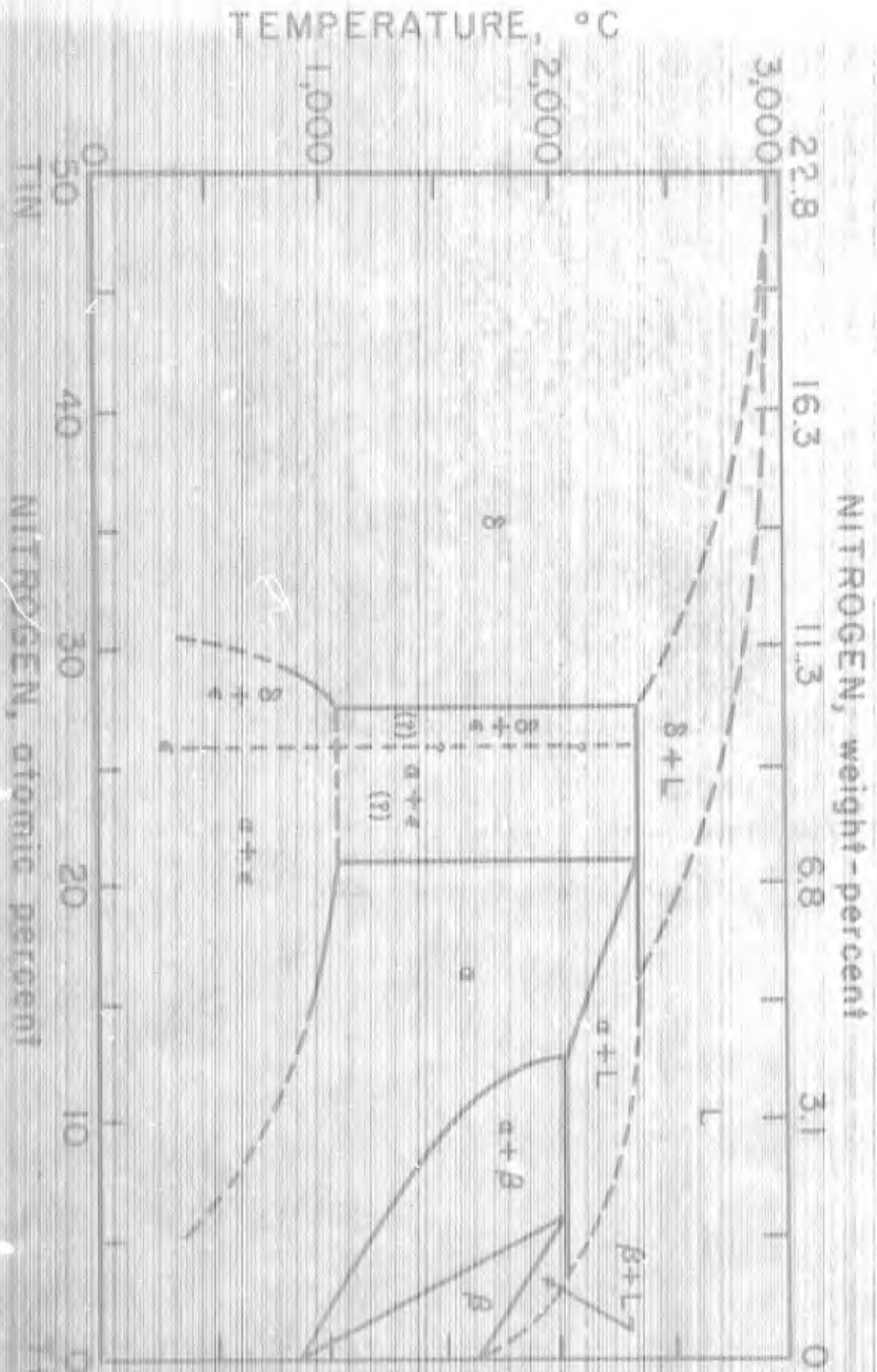


FIGURE 30 - TI-TIN Phase System

NITROGEN, atomic percent

NITROGEN, weight-percent

TEMPERATURE, °C

TIN

alloys, below both liquidus and solidus temperatures of the entire range of Ti-TiN compositions. Nevertheless, depletion of nitrogen at the outside edge of the inclusions, the existence of a reaction zone around the inclusions, and associated porosity all point to some decomposition of the refractory lump in the process of forming a type I defect. It was mentioned in section 3.1 of this report that the delta-phase nitrides lose nitrogen at fusion temperatures. Some of this degassing probably occurs as the lump sinks, especially in the hotter parts of the pool. A mantle of adhering nitrogen should thus be expected, and this should both buoy the lump and insulate it. The reaction zone would then result from solution and diffusion of the liberated nitrogen. In terms of phases, the type I defects range in structural composition from delta plus epsilon in the inclusion core, through an alpha-phase solid solution at the kernel edge, to an alpha plus beta basket-weave in the reaction zone that finally blends with a beta or transformed beta matrix structure.

Although it has been mentioned before, it should be re-emphasized here that there is considerable confusion about phases in the composition range from about 20 to 33 at. % N. Stable existence of the epsilon phase has been reported at temperatures of nearly 1,600° C. Furthermore, the stoichiometry of the epsilon phase has been variously designated as Ti_2N , Ti_3N , and Ti_4N — each with justification. Thus, perhaps the epsilon phase has a different composition than indicated in Figure 38, and perhaps the isothermal boundary near 1,000° C represents only a displacive transformation rather than a reconstructive one. Whatever is the truth, the "epsilon" designation is being used rather loosely in this report.

Since the type I defects seem to be frozen in the process of degassing and dissolution, it is convenient to visualize the type II defects as an extension of the process to the point where the delta and epsilon phases are gone and the remaining heterogeneity encompasses a gradient through the alpha, alpha plus beta, and beta phase regions. Again it should be understood that the beta structure may be of the metastable "transformed" variety.

It is tempting to guess that the type III defects result from a further dissolution of the type I and II inclusions. However, this is difficult to rationalize in terms of the phase system. Instead, it is suggested that the type III defects are essentially equivalent, compositionally, to the type II defects. But whereas the type II defects must be quenched quickly in order to retain the alpha-beta basket-weave, a more retarded thermal history must be presumed for the type III defects. In fact, cooling must be slow enough

for the nitrogen-rich beta phase to revert to the alpha phase, thereby precluding all but traces of the basket-weave structure, and also slow enough for precipitation of epsilon-phase micro-inclusions from that part of the defective regions richest in nitrogen.

3.4 Syntheses of Other Defects

This project (161-6) is not the only work in which syntheses of alpha-stabilized defects have been attempted or accomplished. Unfortunately, little of the other work has been published, and even when published, distribution has been limited. So, it seems worthwhile briefly to review those results that can be repeated.

At the Interper Titanium-Magnesium Plant, in Russia, discolored titanium sponges were selected and used as defect seeds in some 7 kg unalloyed ingots (10). The sponges already have been described in Table II. Only the "grayish-white" oxynitride material containing 4.76 w/o N and 3.17 w/o O, caused discrete defects. Oxidized sponges containing only small amounts of nitrogen apparently dissolved. There was evidence that the oxynitride was reduced to a composition closer to titanium nitride, during melting.

Two investigations have involved syntheses of alpha-stabilized defects in zirconium alloys, analogous to the case of titanium. The earliest of these was reported by the Westinghouse Electric Corporation at its Bettis Plant (12). First, examination of several inclusions found in rolled sheet indicated that the included material was nitrogen rich, sometimes involving oxygen and sometimes involving carbon also. Then the effect of adding zirconium carbonyl seeds to a 12-lb ingot was determined. No discrete inclusions were formed, but a marked grain boundary precipitation occurred. Finally, weld-bead metal, formed by arc welding with carbon electrodes in air, was used as defect seeds. The contaminated metal contained about 1.3 w/o N, 0.12 w/o O, and 0.045 w/o C. This material did cause discrete, but small, inclusions both in a 14-lb ingot and in a button melt. These defects had several characteristics in common with the natural defects. The artificial defects and the natural ones each tended to diffuse away after heat treatments for 24 to 27 hours at temperatures between 1,000 and 1,050° C.

The other work concerning zirconium alloys was described by Imperial Metals Industries, Ltd. of Great Britain in "A Technical Note on Bright-Itching Areas -- November 1960", originally issued confidentially, but declassified in July 1961. After satisfying themselves that the characteristic abnormality of the defects was their high nitrogen content, they first inspected all raw materials for nitrogen contamination. Very little evidence of high nitrogen was found, so it was decided that the raw materials were an unlikely source and attention was turned to weld contamination. They found welds contaminated with up to 2.8 w/o N when welded with a tungsten electrode under a deliberately defective argon shield, and up to 620 ppm N when welded with a tungsten electrode in an enclosed chamber. They succeeded in causing typical defects in nonconsumable button melts when weld metal containing more than 0.2 w/o N was added. But they failed to cause defects in a consumable-electrode melt containing seeds of metal with up to 0.5 w/o N. The dispersion of natural defects by diffusion was not complete enough to avoid serious localized corrosion problems in the defect region. It should be noted that subsequent to this particular investigation, IMI personnel discovered evidence of occasional nitride contamination in zirconium sponge.

Practically all of the alpha-stabilized defect studies in the United States, relating directly to titanium, have been proprietary. The few specific details of this work that are known cannot, in good faith, be revealed. It does seem permissible, however, to comment that the work tends to be consistent with the reasoning presented in sections 2.1A and 2.1B of this report. Artificial defects can be caused by almost any highly refractory oxide or nitride, but nitride-caused defects seem to have more features in common with most of the natural defects, and the best agreement seems to result when nitrides of titanium itself are involved.

4. DEFECT SURVIVAL IN MELTING

4.1 Unalloyed Ingots

Unalloyed ingots were melted under the conditions given in Table XII. This group of experiments was planned primarily to indicate the effects of arc current and pressure variations. Nevertheless, an electroslag melt was included also. Ingot 25,936 was promptly remelted into ingot 25,951, and ingots 25,937 and 25,951 were then extensively cut up to obtain representative specimens of defects. Defects in the rest of the ingots were examined in situ using the single-cut evaluation technique described in section 3.2 of this report.

Cross sections of two ingots in as-cast and etched conditions are shown in Figures 39 through 42. Unfortunately, in this study, a way of illustrating all defects with photographs has not been found. Most contrasts apparent to the eye are obscure in photos. Only relatively large type I defects show up. The polished surfaces behave too much like mirrors and the grain structure brought out by etching tends to mask the defect details. Therefore, in order to display the comparative defectiveness of ingots, an arbitrary scoring scheme was used. Type I defects were assigned values of 10, 25, 50, or 100 points depending on whether they were small, medium, large, or huge respectively. The inclusion that can be seen in Figure 39 was classified as large. Only one defect was considered huge. Type II defects were assigned values of 5 points each, and type III defects were scored at 2 points each.

The results of arbitrary defectiveness scoring are presented in Table XIII. Reference to Table XII reveals that the group of ingots 25,941, 2, 4, and 5, and the group 25,947, 8, 39, and 40 each represent a series of arc currents in increasing order, but that different atmospheres were used in the furnace in each case. The most definite trend implied is a decrease of defectiveness at the higher currents. Considering the difficulty in evaluating type III defects in the ingots melted in inert gas, it is apparent also that better ingots were produced in a vacuum environment, especially with regard to type I defects. Results of the electroslag-melting experiment were not very encouraging. In the remelt ingot, there seemed to be a shift of defects from type I to type III. Overall, the best ingot resulted from the use of the highest arc current and a vacuum environment.

TABLE XII. - Unalloyed Ingots

Number	Crucible diam., inches	Melt type 1/	Nominal current, amps.	Furnace gas	Estimated pressure at melt, torr	Hardness, rhn		As-cast weight, kg
						Top	Bottom	
25, 936	3	F, A	1, 200	vac.	15 2/	-	-	2.86
25, 937	3	F, A	1, 700	vac.	15 2/	-	-	2.25
25, 947	3	F, A	1, 500	vac.	15 2/	B52	B52	2.30
25, 948	3	F, A	1, 700	vac.	15 2/	B52	B50	2.40
25, 939	3	F, A	2, 200	vac.	15 2/	B78	B80	2.35
25, 940	3	F, A	2, 700	vac.	15 2/	B75	B76	2.30
25, 941	3	F, A	1, 200	He	400	B72	B33	2.15
25, 942	3	F, A	1, 700	He	400	B63	B74	2.30
25, 944	3	F, A	2, 200	He	400	B76	B80	2.30
25, 945	3	F, A	2, 700	He	400	B66	B75	2.40
25, 961	3	F, E	2, 400	He	300	-	-	2.70
25, 951	3	R, A	2, 400	vac.	10 2/	-	-	2.00
25, 285	4	R, A	5, 600	vac.	2 2/	-	-	7.30

1/ Symbols: F - first melt, R - remelt, A - consumable-electrode arc melt, E - consumable-electrode electrolytic melt.

2/ Dynamic vacuum maintained with 27 CFM, 1-stage pump.

3/ Dynamic vacuum maintained with 1, 100 CFM lobe-type blower.

TABLE XIII - Defectiveness Scores for Unalloyed Castings

Lot	Defectiveness Score			Total	Remarks
	Type I	Type II	Type III		
25, 941	130	10	1/	130 1/	avg first melt, inert gas
25, 942	110	0	1/	110 1/	Do.
25, 944	85	0	1/	85 1/	Do.
25, 945	85	15	1/	100 1/	Do.
25, 947	75	25	14	114	are first melt, vacuum
25, 948	80	60	40	180	Do.
25, 959	60	60	0	110	Do.
25, 940	0	60	8	68	Do.
25, 551	175	25	4	204	electroslag first melt
25, 235	50	25	26	101	are remelt of 25, 941, 2, 4, and 5

1/ Too porous for evaluation of type III defects.

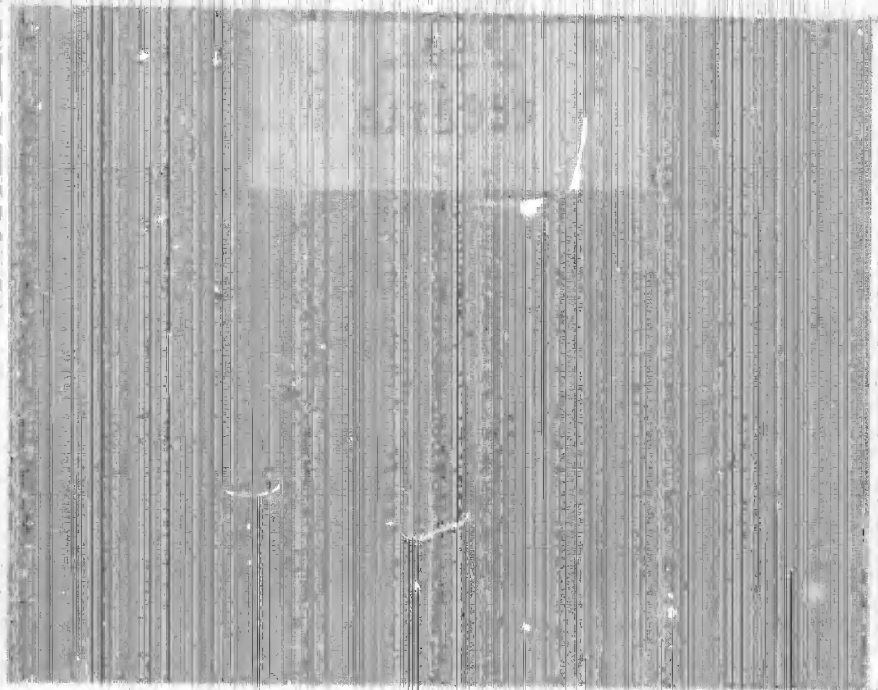


Figure 39. Ingot of unalloyed Ti, melted at 2,200 amp, in dynamic vacuum with defects induced artificially.



Figure 40. Ingot of unalloyed Ti, melted at 2,740 amp, in dynamic vacuum with defects induced artificially.

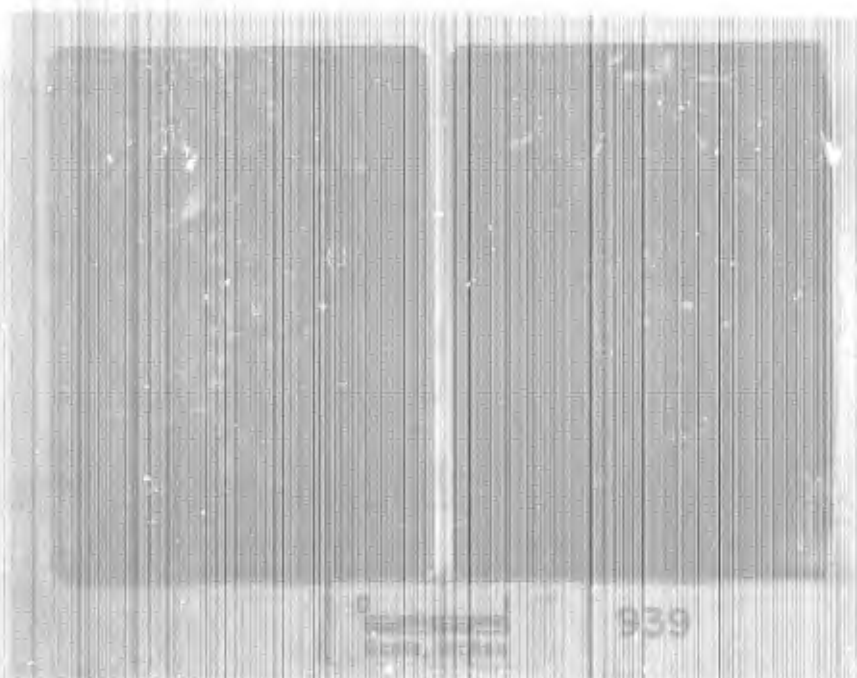


Figure 41. Ingot shown in Figure 39, after etching.

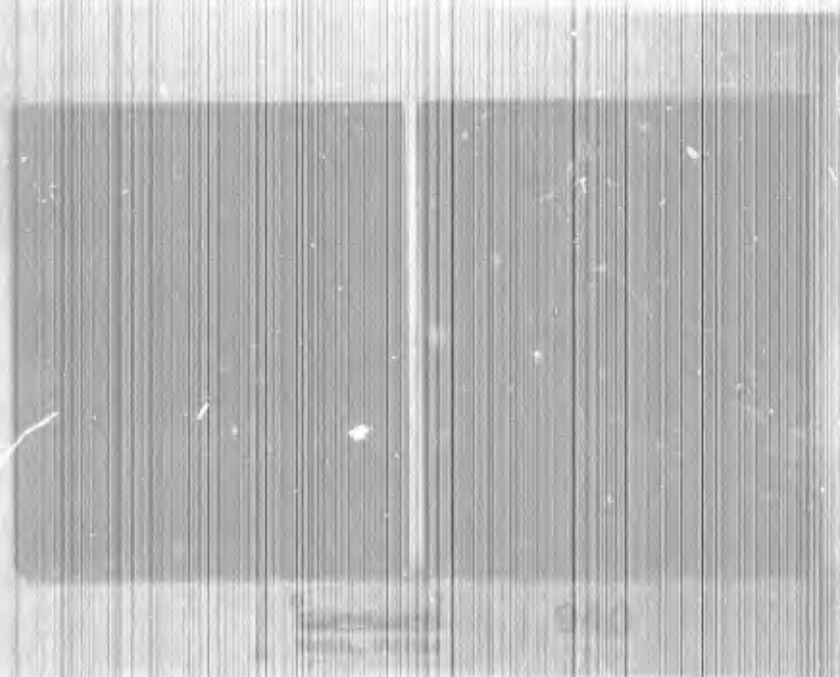


Figure 42. Ingot shown in Figure 40, after etching.

4.2 Ti-6Al-4V Alloy Ingots

Studies of the effects of melting conditions were continued, using Ti-6Al-4V alloy metal as the host for artificial defects. Four arc first melts are shown in Figure 43. An electroslag first melt is shown in Figure 44. Melting conditions for the entire group are summarized in Table XIV. Following the experience with unalloyed ingots, a relatively high current and a vacuum environment were selected as basic control conditions for alloy melting. Magnetic stirring, pneumatic vibration, and skull casting were the new variations introduced, and the effects of vacuum enhancement, electroslag melting, and remelting were explored some more.

Ingots 26,406 and 26,409 were set aside for some rolling tests that still remain to be done, and all other ingots were subjected to the single-cut evaluation. A collection of several cut ingots in as-polished condition is shown in Figure 45, and a close-up view of ingot 26,257 appears in Figure 46. Etched cross sections of selected "good" and "bad" ingots are illustrated in Figures 47 through 52.

The results of evaluation are listed in Table XV. The advantage of remelting was clearly demonstrated in the alloy melting. It seems that special efforts to enhance the vacuum may be of some value, but the effect is not clearcut. The result of electroslag melting was some better than obtained previously on a smaller scale, but it still does not seem to be an efficient way to dissolve nitrogen-rich refractories. Electromagnetic stirring failed to cause improvement and it may have been detrimental. It was noticed that type I defects in the ingots that were stirred as they melted were distributed more uniformly along the length rather than being concentrated toward the bottoms of ingots. The most hopeful results of alloy ingot melting were connected with the use of pneumatic vibration and the skull-casting technique, especially the latter. The vibration, when combined with remelting, may have eliminated type I defects in at least two cases. However, on the basis of 3 tests, the skull-casting practice seems to have avoided both type I and type II defects in both first-melt and remelt ingots.

As a further test of the effect of skull casting, one-half of ingot 26,257 was sliced into 11 D-shaped sections by cutting laterally. Starting with 2,307 grams, 662 grams were lost in cuts that averaged 0.37 cm in thickness. The effective discovery thickness of each cut was $(t + d)$ where t = the 0.37 cm thickness and d = the dimension of a particular defect. An

TABLE XIV. - Ti-6Al-4V Alloy Ingots

Number	Crucible or Mold diam., inches	Melt Type 1/	As-cast Weight, kg	Deviations from Basic Conditions 2/	
25, 194	5	F, A	19.0	none	
25, 195	5	F, A	18.1	none	
25, 205	5	F, A	18.75	magnetic stirring used	
25, 206	5	F, A	20.0	Do.	
25, 209	5	F, A	18.5	pneumatic vibrator operated	
25, 212	5	F, A	19.4	Do.	
25, 220	5	F, A	19.9	vacuum enhanced by use of 1,100 CFM lobe-type blower, estimated pressure at melt - 1 to 2 torr	
26, 214	6	F, E	21.1	CaF ₂ slag plus 250-300 torr of He present, 6500 to 6600 amps of current	
26, 257	4	F, S	4.9	skull cast, over the lip, vacuum enhanced	
26, 405	5	R, A	15.7	only 3,400 amperes nominal current	
26, 409	5	R, A	12.1	air leak developed near end of melt - some discoloration of ingot	
26, 406	5	R, A	15.2	none	
26, 420	5	R, A	15.5	none	
26, 412	5	R, A	16.6	pneumatic vibrator operated	
26, 415	5	R, A	15.95	Do.	
26, 421	5	R, A	15.45	vacuum enhanced by use of 1,100 CFM lobe-type blower, estimated pressure at melt - 0.5 torr	
26, 424	4	R, S	5.6	skull cast, over the lip, vacuum enhanced	
26, 427	4	R, S	5.3	Do.	

1/ Symbols: F - first melt, R - remelt, A - consumable-electrode arc melt,

E - consumable-electrode electrosag melt, S - consumable-electrode arc melted and skull cast,

2/ Basic conditions comprised 5,500 amperes and the use of a 27-CFM single-stage rotary-piston vacuum pump that achieved pressures estimated as 10 to 20 torr at the melt.

TABLE XV. - Defectiveness Scores for Ti-6Al-4V Ingots

Ingot	Defectiveness Score			Total	Remarks
	Type I	Type II	Type III		
26, 194	100	40	0	140	arc first melt, control conditions
26, 195	85	45	16	146	Do.
26, 205	90	60	0	150	arc first melt, control conditions plus magnetic stirring
26, 206	135	60	24	209	Do.
26, 209	25	5	0	30	arc first melt, control conditions plus vibration
26, 212	60	30	2	92	Do.
26, 220	35	10	10	55	arc first melt, control conditions except enhanced vacuum
26, 214	100	30	0	130	electroslag first melt
26, 257	0	0	8	8	arc first melt, skull cast
26, 406	20	30	8	58	arc remelt of 26, 195, control conditions
26, 420	0	25	16	41	arc remelt of 26, 206, control conditions
26, 421	55	15	12	82	arc remelt of 26, 220, control conditions except enhanced vacuum
26, 413	0	20	10	30	arc remelt of 26, 212, control conditions plus vibration
26, 415	0	15	14	29	arc remelt of 26, 205, control conditions plus vibration
26, 424	0	0	6	6	arc remelt of half of 26, 214, skull cast
26, 427	0	0	10	10	Do.

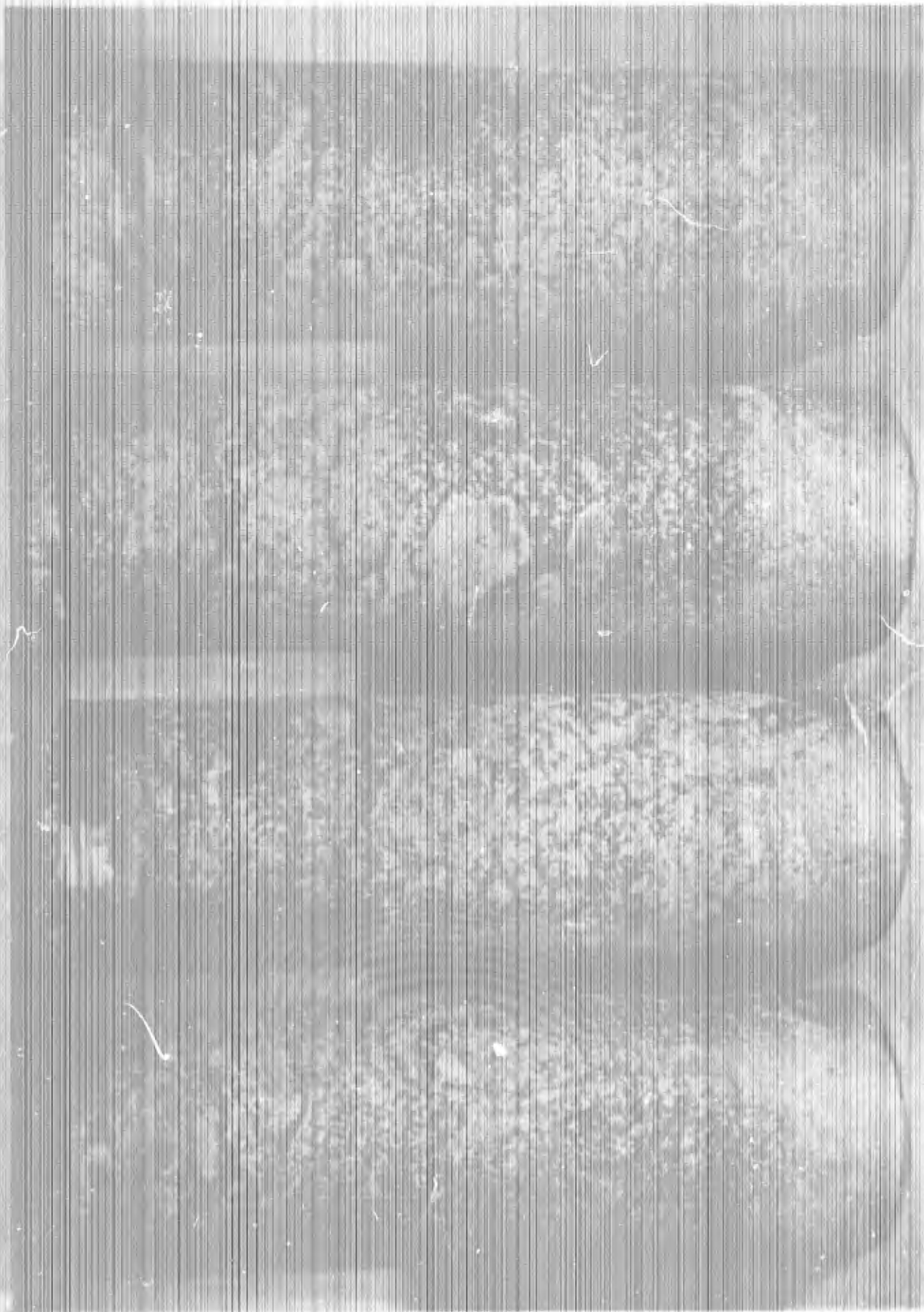


Figure 43. Typical 5-inch arc-melted ingots of Ti-6Al-4V alloy, containing artificial defects, as-cast condition.



Figure 44. Six-inch electric-arc-melted ingot to which defect seeds were added.



Figure 45. Some defective ingots after cutting and polishing for evaluation.



Figure 46. Close-up view of a small-cast ingot apparently free of types I and II alpha-stabilized defects.

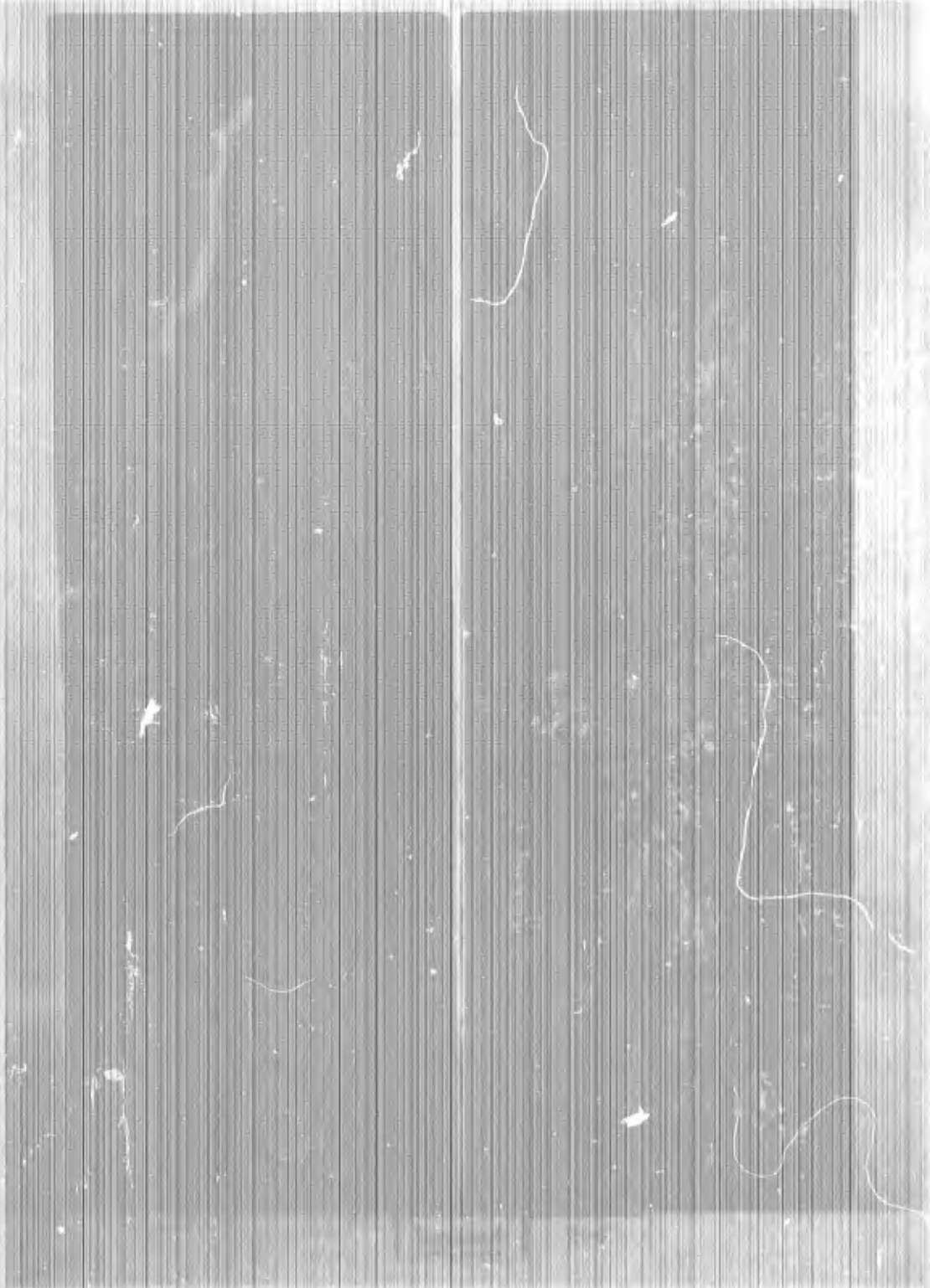


Figure 47. Etched cross section of ingot SA 28,206.

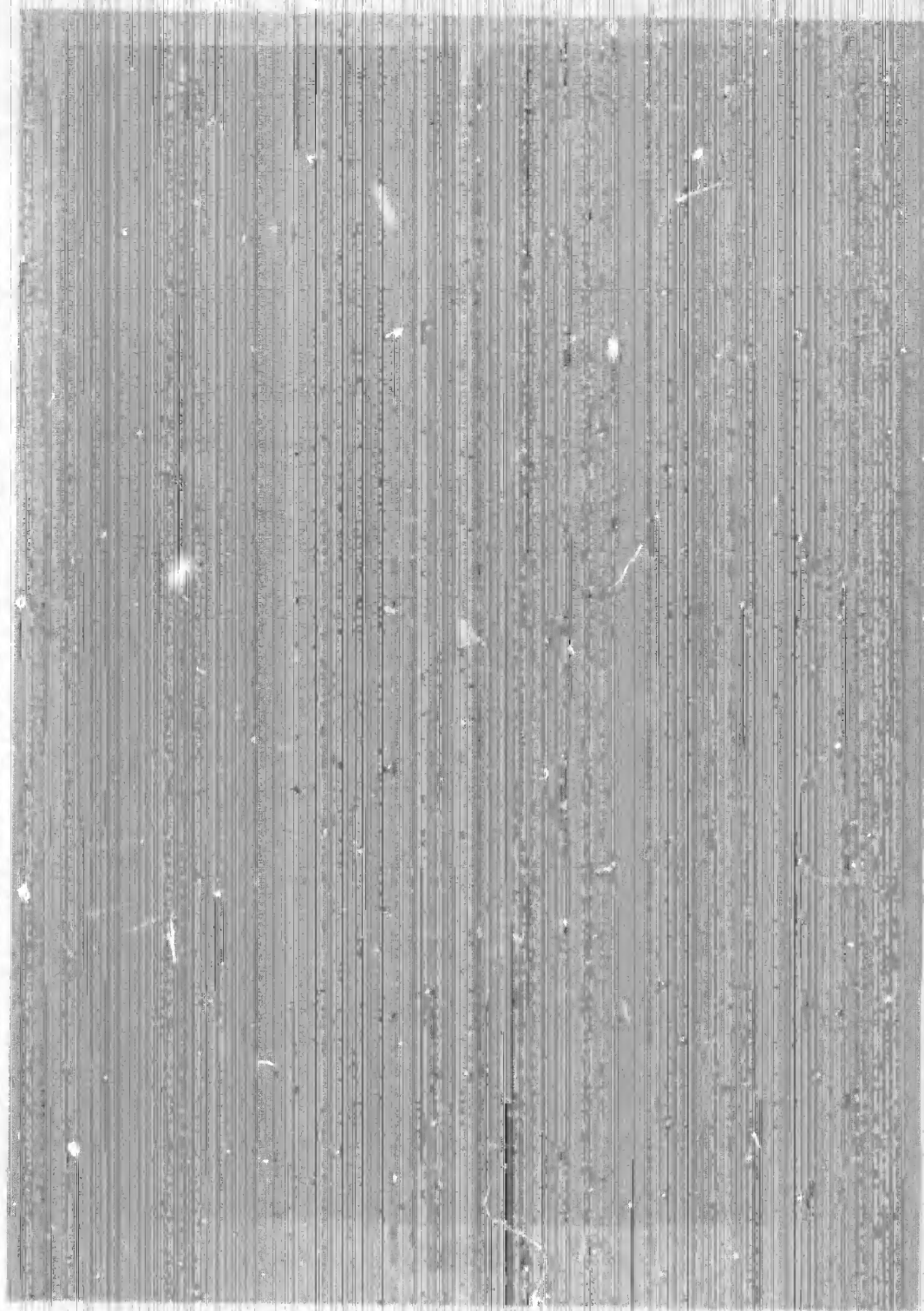


Figure 48. Etched cross section of Ingot SA 26, 220.

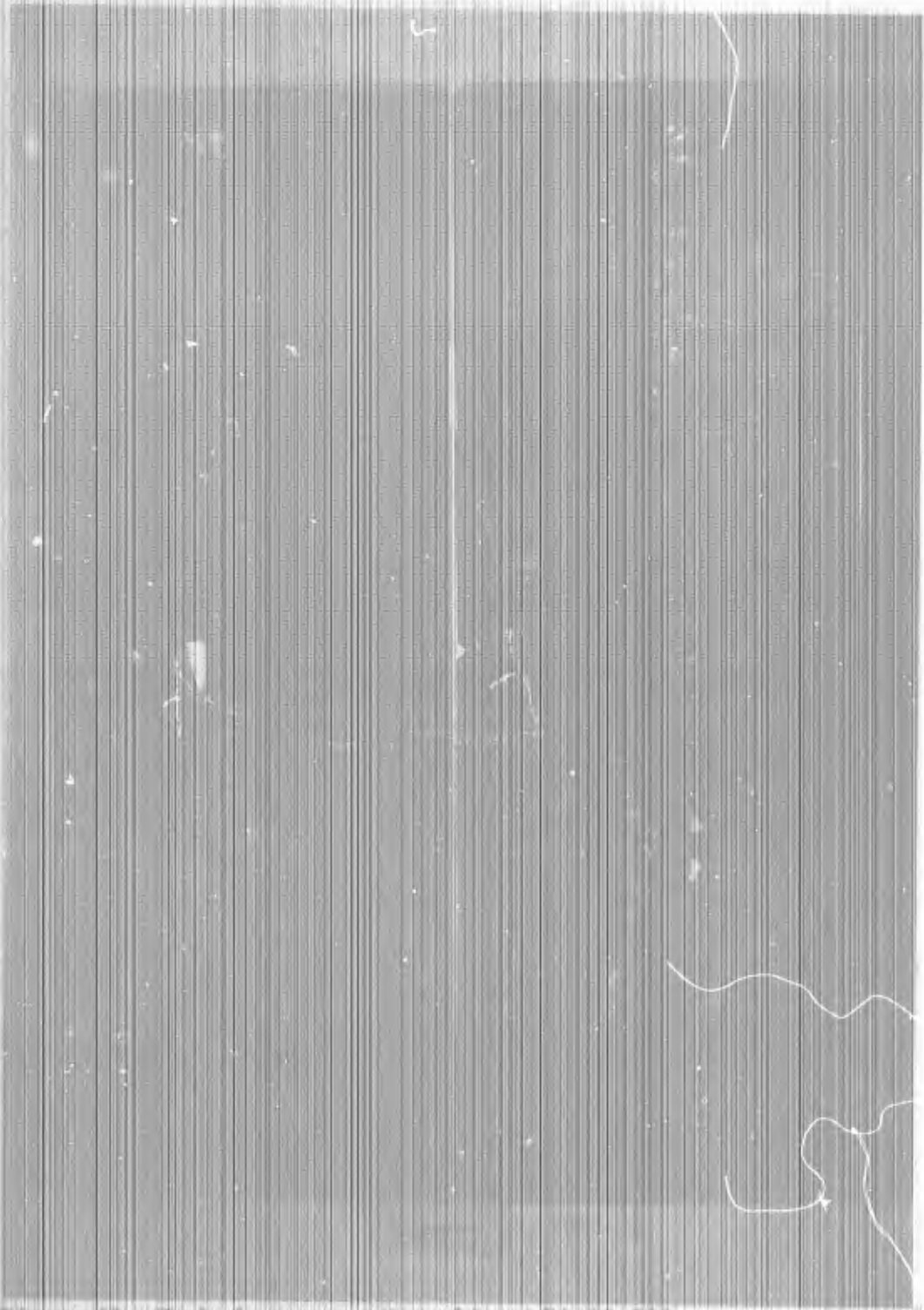


Figure 49. Etched cross section of ingot SA 26,209.



Figure 50. Etched cross section of ingot SA 26, 257.

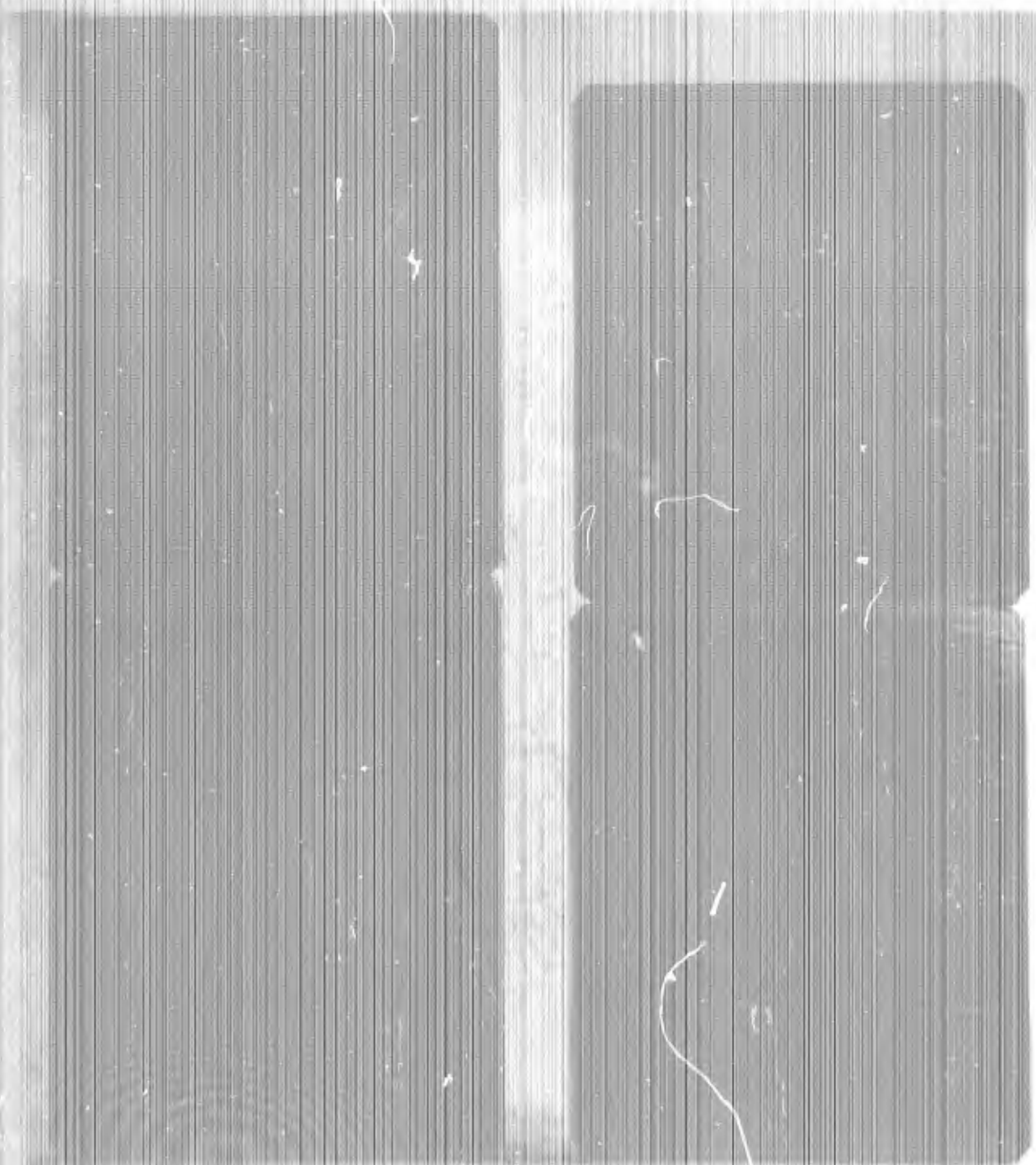


Figure 51. - Etched cross sections of ingots SA 26, 412 (left) and SA 26, 421 (right).



Figure 32. Etched cross section of ingot SA 26, 434.

approximation for the chance that a defect of any particular size was encountered is $P = [d + N(\pi + 3)] / L$, where N is the number of cuts, and L is the original length. In the present case, it turns out that P varied from a minimum of 27 percent for vanishingly small defects, to 50 percent for $d = 0.23 \mu\text{m}$, to 100 percent for $d = 0.91 \mu\text{m}$ or larger. Each D-shaped section was polished in a search for defects at the surfaces. None of type I or II were found, although a few more of type III were revealed.

4.3 Discussion

Results of the high-melting experiments contain some logical consistency. The indications of its success in dissolving refractory nitrides increases when the D to the refractory material is exposed to molten metal in hot metal, when turbulence is imparted to the hot and/or solidifying metal, and when the rate of solidification is retarded. Notice, however, that these factors are interrelated, and that the rate of solidification is not necessarily the same as the rate of melting.

The main ways in which the time factor was increased were to generate a deep molten pool so the refractory material had a long distance to sink before reaching solid metal, and simply to repeat the melting process so the refractory material was re-exposed. Deep molten pools are caused by rapid melting (hence high current input) in a vacuum environment. In cold-chamber melting the molten pool grows in volume (and interfacial surface area) as long as the melting rate exceeds the rate of solidification, and the faster the melting, the longer it takes for solidification to catch up, and the greater the steady-state volume will be. Alternatively, slow solidification progress during melting also prolongs the attainment of a steady state. The vacuum environment influences pool volume through at least two interactions. The heat distribution in an electric arc depends on the pressure of the conducting gaseous medium. Thus the rate of melting is maximum, for a particular power input, at some low pressure (40). Heat transfer away from a cold-chamber ingot during melting depends, in part, on the effective thermal transmittance across the shrinkage gap that forms between the ingot wall and the crucible. Because vacuum is a rather good insulator, solidification is retarded when the shrinkage space is evacuated.

Whether the molten pool is large or not, it is advantageous after melting to solidify the metal slowly, so any suspended refractory lumps will dwell in molten metal for the longest possible time. A vacuum environment

probably helped in this way, again by operating as an insulator in the shrinkage gap. But the most significant invocation of slow cooling probably occurred in the skull-casting experiments when the molten metal was transferred from chilled copper to a graphite mold to solidify.

Reasons for the effect of turbulence are quite speculative. One possibility is that the suspension of particles in the pool is enhanced so that the downward gravitational drift of the refractory lumps is slowed or interrupted. Another possibility is that the gas mantle that probably adheres to the decomposing particle is disrupted and dispersed, thereby accelerating dissolution of the refractory matter. In any case, in the experiments being discussed, the greatest turbulence resulted from over-the-lip skull casting. Next, in magnitude of turbulence were the experiments with pneumatic vibration. The molten pools in the experiments with magnetic stirring were not particularly turbulent. Instead, the action in those cases was a relatively smooth centrifugal circulation. Thus, the likely consequences of magnetic stirring were thermal homogenization of the pool and improvement of thermal contact at the perimeter of the pool surface by slight vortexing and washing against the crucible. Undoubtedly, turbulence can be magnetically generated by using an alternating current in a solenoid to rapidly reverse the stirring direction. However, agitation of molten pools on a fully industrial scale by either magnetic or mechanical means is known to be difficult to implement, and chances are slim that the approach would be a practical solution to the problem of alpha-stabilized defects, even if complete elimination had been demonstrated.

A combined effect of long exposure, slow solidification, and turbulence was to cause differences in ingot macrostructure that seemed to go along with reductions in defectiveness. In part, it is the purpose of Figures 41, 42, and 47 through 52 to illustrate this feature. The skull-cast ingots shown in Figures 50 and 52 are obviously and understandably different. The main point of difference is the generally equiaxed character of the structure. Among the cold-mold ingots, differences are more subtle. In each case, the structure is columnar near outside surfaces and more nearly equiaxed in a core region. But the trend is for the better ingots (see Tables XIII and XIV) to exhibit an equiaxed core that is greater in longitudinal extent and more uniform in lateral extent, and also to have a less pronounced longitudinal component of orientation among columnar grains. The differences of structure undoubtedly result from thermal differences.

Overall, the best procedure for eliminating alpha-stabilized defects appears to be incorporation of skull casting in a two-stage melting sequence. There are several reasons for avoiding skull casting as a remelting method. Two significant ones are the limited scale (less than a half ton) on which skull casting is usually practiced, and the lack of a satisfactory hot-topping procedure in skull casting. Therefore, it is more appropriate to consider skull casting in the first stage of melting. The technical and economic practicalities of the idea must each be tested in pilot operations. Certainly, the suggestion would involve added costs, but alpha-stabilized defects will not be eliminated without some expense, regardless of how it is done. Any judgment of economic implications should await the outcome of a careful cost study.

Another objection that might be anticipated is that present skull-casting capacity would be far short of requirements for primary metal production, so that a capital investment in new plant would be required. But differences in cold-chill arc-melting furnaces and skull-casting furnaces are not great, and it may well be possible to convert most existing first-melt furnaces to skull-casting furnaces with relatively little delay or expense. Again, the matter deserves some study.

Among approaches not tried in this investigation are triple melting, electron-bombardment melting, and the use of trace additives to alloys to enhance the solubility of nitrides in molten metal. Triple melting would undoubtedly be advantageous, but it too would have some disadvantages, and it too would be over more effective if the first stage of melting were skull casting. Electron-bombardment melting is characterized by comparatively slow melting rates and shallow molten pools. The experience with arc and electroslag melting indicates that these conditions do not favor defect elimination. Nevertheless, the method should be tested to be sure that other factors are not overriding. The question of solubility-modifying additives is a complex one that would probably require an extensive and comprehensive investigation by itself. In general, it might be expected that solubility should be enhanced by raising the melting temperature of the solvent, or by reducing the melting temperature of the solute. The second alternative, by forming low-melting intermediate phases, is probably more consistent with additions of trace amounts. Among remote possibilities that could be examined are yttrium and the lanthanide metals.

5. CONCLUSIONS AND RECOMMENDATIONS

No direct evidence was obtained to link alpha-stabilized defects with any specific sources or causes. Nevertheless, direct evidence did show that a major number of defects were composed of refractory "nitrides". Indirect arguments and results indicate several possible sources for both nitrides and other refractory substances. Among these possibilities, the nitrides are the most refractory, so that procedures eliminating them will probably eliminate defects of other compositions as well.

Tests with artificial nitride defects revealed that the flaws are manifested in three forms depending on the degree of decomposition and dissolution, and on thermal conditions. It was also learned that the interrelated factors of exposure time, melt turbulence, and solidification rate are most influential in reducing the survival of nitrides during melting. Of various melting schemes tried, skull casting was most effective in maintaining the conditions that discouraged defect survival. High arc current, a vacuum environment, remelting, and mechanical vibration of the melt were also beneficial. No advantage was demonstrated for unidirectional magnetic stirring of arc melts or for electroslag melting.

It is recommended that the success of skull casting in eliminating artificial alpha-stabilized defects be tested by using the method as the first stage of melting in two-stage vacuum-arc melting. This should be done on a semi-commercial scale at least, with emphasis on technical details and problems. Other matters that need more investigation include the effects of deformation and annealing on alpha-stabilized defects.

6. REFERENCES

1. Agayev, N. V., and M. S. Model. (Determination of the Concentration of Gaseous Impurities in Titanium from the Magnitude of the Lattice Constants.) *Zhur. Neorg. Khim.*, vol. 3, 1958, pp. 1439-46.
2. Anzures, S. L., and E. A. Beall. Electroslag Melting of Titanium Slabs. In: *Transactions of the International Vacuum Metallurgy Conference 1967*, E. L. Foster, ed., Am. Vac. Soc., New York, 1968, pp. 675-694.
3. Azarov, L. V. *Introduction to Solids*. McGraw-Hill, New York, 1960, 460 pp.
4. Baroch, J. T., T. B. Kaczmarek, W. D. Barnes, L. W. Galloway, W. M. Mark, and G. A. Lee. *Titanium Plant at Boulder City, Nev.: Its Design and Operation*. U.S. Bureau of Mines Report of Investigations RI 5141, Sept. 1955, 78 pp.
5. Beall, R. A. *Cold-Chold Arc Melting and Casting*. Bureau of Mines Bulletin 666, U.S. Government Printing Office, Washington, D. C., 1962, 157 pp.
6. *Chemical Engineering*. Sodium Proves Cheap Key to Unlock Titanium. Oct. 9, 1961, pp. 126-8.
7. Chisolm, D. S., and W. F. Saunders. *Method of Treating Molten Magnesium*. U.S. Patent 2,779,672, Jan. 29, 1957.
8. Collongues, R., J. C. Gilles, A. M. Lajus, M. Pavez y Jorba, and

- D. Michel. Recherches sur les Concentrations Metalliques. Mat. Res. Bull., vol. 2, no. 9, 1967, pp. 637-43.
8. Evans, R. C. An Introduction to Crystal Chemistry, 2nd ed., Cambridge Univ. Press, 1966, 410 pp.
10. Faltevizh, E. S., Ye. A. Lyukovich, and A. N. Kucharenko. (On the Problem of Defective Inclusions in Titanium Ingots.) In: Physical Metallurgy of Titanium, I. I. Kornilov, ed., Science Publishing House, Moscow, 1964. NASA Translation TT F-338, Nov. 1965, or WPAFB Foreign Technology Div. Translation HT-66-354, Dec. 1966.
11. Grala, E. M. Characterization of Alpha Segregation Defects in Ti-6Al-4V Alloy. Interim Report IR-7351 (1), TRW Inc. to AFML(MAMP), Nov. 1967, 27 pp.
12. Crozier, J. D. Inclusion Problem in Zircaloy-2. In: Zirconium Highlights, Rept. No. WAPD-ZH-11, Westinghouse Elec. Corp., Pittsburgh, Penn., October 1958, pp. 2-8.
13. Gulbransen, E. A., and K. F. Andrew. Kinetics of the Reactions of Titanium with O_2 , N_2 , and H_2 . Trans. AIME, vol. 185, Oct. 1949, pp. 741-8.
14. Hansen, M., and Anderko. Constitution of Binary Alloys, 2nd ed., McGraw-Hill, New York, 1958, 1,305 pp; also 1st supplement by R. P. Elliott, 1965.

15. Higbie, K. B., and J. W. Stamper. The Production of Primary Titanium Metal. In: Titanium for the Chemical Engineer, DMIC Memo. 234, Battelle Memorial Inst., Columbus, Ohio, April, 1968, pp. 8-12.
16. Holmberg, B. Structural Studies on the Titanium-Nitrogen System. *Acta Chem. Scand.*, vol. 16, 1962, pp. 1255-61.
17. Sultgren, R., H. I. Orr, P. D. Anderson, and K. E. Kelley. Selected Values of Thermodynamic Properties of Metals and Alloys. John Wiley and Sons, New York, 1968, 963 pp. and supplementary data sheets.
18. Klempner, E. K., and T. A. Henrie. Preparation of Titanium Nitride. U. S. Bureau of Mines Report of Investigations RI 6447, 1964, 8 pp.
19. Kranke, F. J., J. W. Hays, and D. L. Spell. High Purity Electrolytic Magnesium. *J. Metals*, vol. 10, no. 1, Jan. 1958, pp. 28-30.
20. Kroll, W. J. Titanium. *Metal Industry*, August 5, 1955, pp. 105-8.
21. Mokshanova, E. K. Phase Diagrams of Titanium Alloys. Daniel Davey and Co., Inc., New York, 1965, 296 pp.
22. Naga, T. Titanium From Slag in Japan. *J. Metals*, vol. 17, no. 1, Jan. 1965, pp. 26-32.
23. Ferraro, W. B. Comments on "Evidence of Metallic Bonding in TiN." *Acta Met.*, vol. 10, 1962, p. 1122.

24. Reussback, B. F., W. C. Coors, and R. A. Perkins. High-Temperature Stability of Epitaxial Ti_xN . *Trans. AIME*, vol. 242, Feb. 1966, pp. 345-5.
25. Houkin, M. P., and J. M. Paris. *1960's Binary and Ternary Solutions Between Nitrides and Oxynitrides of Chromium, Vanadium, and Titanium.* *Compt. Rend. Acad. Sci., Paris, Ser. C*, vol. 263, no. 22, 1966, pp. 1381-4.
26. Samsonov, G. V., T. S. Verkhoglyadova, M. M. Antonova, and T. V. Dubov'ka. (Preparation of Nitrides of Refractory Metals.) Cited in *Chem. Abstr.*, vol. 56, 1962, abstr. no. 32301.
27. Samsonov, G. V., T. S. Verkhoglyadova, S. N. Lvov, and V. F. Semchenko. (The Influence of Oxygen on the Electric Properties of Titanium Nitride.) *Dokl. Akad. Nauk SSSR*, vol. 142, no. 4, 1962, pp. 862-5.
28. Schmitz-Dumont, G., and K. Stohberg. *Mischkristallbildung im System TiO-TiN.* *Naturwiss.*, vol. 41, no. 5, 1954, p. 117.
29. Schofield, F. H., and A. R. Bacon. The Melting Point of Titanium. *J. Inst. Metals*, vol. 52, no. 4, Dec. 1953, pp. 167-8.
30. Stokes, C. S. Chemical Reactions with the Plasma Jet. *Chem. Engineering*, vol. 72, April 12, 1958, pp. 191-6.
31. Stone, L., and H. Margolin. Titanium-Rich Regions of the Ti-C-N, Ti-C-O, and Ti-N-O Phase Diagrams. *J. Metals*, vol. 5, no. 11, Nov. 1953, pp. 1498-502.

32. Skoll, D. R., and others. JANAF Thermochemical Tables. Dow Chem. Co., Air Force Contract AF 64 (611) - 7554, through the Clearinghouse, Dept. of Commerce, August 1965, pages unnumbered with allowance for supplements.
33. Viskarev, A. V., A. Z. Andreev, and V. Rodyakin. (Refining Magnesium with Titanium Tetrachloride Vapors.) Soviet J. of Nonferrous Metals (English Transl.), vol. 7, no. 6, June 1966, pp. 61-2.
34. Wartman, F.S., D.H. Baker, J.E. Nettle, and V.E. Homme. Some Observations on the Kroll Process for Titanium. J. Electrochem. Soc., vol. 101, no. 10, Oct. 1954, pp. 507-13.
35. Wasilewski, R. L., and G. L. Kehi. Diffusion of Nitrogen and Oxygen in Titanium. J. Inst. Metals, vol. 83, Nov. 1954, pp. 94-104.
36. Westbrook, J. E., ed., Intermetallic Compounds. John Wiley and Sons, New York, 1967, 663 pp.
37. Wicks, C. E., and F. E. Block. Thermodynamic Properties of 65 Elements - Their Oxides, Halides, Carbides, and Nitrides. Bureau of Mines Bulletin 605, U. S. Gov't Printing Office, 1963, 146 pp.
38. Wood, F. W. A Model for Molten Pools in Arc Melting. U.S. Bureau of Mines Report of Investigations, RI 7151, July 1968, 38 pp.

39. Wood, F.W., S. L. Ausmus, and E. D. Calvert. A Casting Technology for Reactive Metals. Modern Castings, vol. 34, no. 1, July 1958. pp. 30-6; also Trans. A. F. S. for 1958, pp. 334-60.
40. Wood, F.W. and R. A. Beall. Studies of High-Current Metallic Arcs. Bureau of Mines Bulletin 625, U. S. Government Printing Office, Washington, D. C., 1965, 84 pp.

UNCLASSIFIED

FORM 10-68

DOCUMENT CONTROL DATA - R 1 1

Security classification of this data and associated information shall be entered when the control system is established. This report is classified UNCLASSIFIED.

Alloy Metallurgy Research Center

U. S. Bureau of Mines

P. O. Box 70, Albany, Oregon 97321

Unclassified

EX GROUP

W/A

Minimization of Low-Density Inclusions in Titanium Alloy Ingots

Approved for release by NSA on 05-08-2014 pursuant to E.O. 13526

Final Technical Report, September 1967 - December 1968.

Approved for release by NSA on 05-08-2014 pursuant to E.O. 13526

Wood, Floyd W.

REPORT DATE

April 1969

REPORT NUMBER

DTIC-68-11-0002

PROJECT NO.

62-1

4

10. TOTAL NO. OF PAGES

86

79. NO. OF REFS

40

11. OPERATOR'S REPORT NUMBER(S)

AFML-TR-69-67

12. OTHER REPORT NO(S) (If available, include report number and report title)

None

13. CONTROLLING AGENCY

This document is subject to special export controls and each transmittal to foreign governments or foreign nationals may be made only with prior approval of the Manufacturing Technology Division of the Air Force Materials Laboratory, Wright-Patterson Air Force Base, Ohio 45433.

14. DISTRIBUTION STATEMENT

15. OPERATIONAL ACTIVITY

Air Force Materials Laboratory (MATT)
Wright-Patterson AFB, Ohio 45433

16. SUMMARY

The problem of alpha-stabilized defects in ingots and billets of titanium and its alloys was investigated. Possible origins were considered, several naturally-occurring defects were studied, and contamination by attrition was selected as a cause needing further investigation. Nitride defects were synthesized and in ingots. Their nature and behavior during melting, casting, and subsequent rolling were explored, and elimination of the artificial defects was attempted by means of melting-process variables. Nitride defect seeds survived melting in three forms, which consistent with the Ti-O₂ phase system if different thermal exposures during melting, solidification, and cooling are assumed. In cold-mold arc melting trials, factors that tended to alleviate ingot defectiveness were good vacuum, high arc current, remelting, and pneumatic vibration of the melt. Only variations used were unidirectional magnetic stirring and electrodeless melting. Improvements obtained by varying the cold-mold practice were generally not good enough. However, reasonable preliminary success was achieved by adopting skull casting as the melting practice. More extensive evaluation of this technique is recommended.

DD FORM 1473

REPLACES FORM 10-68, WHICH IS OBSOLETE FROM 1 JAN 69

UNCLASSIFIED

Security Classification

UNCLASSIFIED

Security Classification

KEY WORDS	LINK A		LINK B		LINK C	
	NOLE	WT	NOLE	WT	NOLE	WT
Metallurgy and Metallography Nitride inclusions and other defects Titanium Titanium alloys Melting and solidification Ti-N phase system						

INSTRUCTIONS

1. ORIGINATING ACTIVITY: Enter the name and address of the contractor, subcontractor, grantee, Department of Defense activity or other organization (Corporate address) issuing the report.

2a. REPORT SECURITY CLASSIFICATION: Enter the overall security classification of the report. Indicate whether "Restricted Data" is included. Marking is to be in accordance with appropriate security regulations.

2b. GROUP: Automatic downgrading is specified in DoD Directive 5200.10 and Armed Forces Industrial Manual. Enter the group number. Also, when applicable, show that special markings have been used for Group 2 and Group 4 as authorized.

3. REPORT TITLE: Enter the complete report title in all capital letters. Titles in all caps should be unclassified. If a meaningful title cannot be selected without classification, show title classification in all capitals in parentheses immediately following the title.

4. DESCRIPTIVE NOTES: If appropriate, enter the type of report, e.g., interim, progress, summary, annual, or final. Give the inclusive dates when a specific reporting period is covered.

5. AUTHOR(S): Enter the name(s) of author(s) as shown on or in the report. Enter last name, first name, middle initial. If military, show rank and branch of service. The name of the principal author is an absolute minimum requirement.

6. REPORT DATE: Enter the date of the report as day, month, year, or month, year. If more than one date appears on the report, use date of publication.

7a. TOTAL NUMBER OF PAGES: The total page count should follow normal pagination procedures, i.e., enter the number of pages containing information.

7b. NUMBER OF REFERENCES: Enter the total number of references cited in the report.

8a. CONTRACT OR GRANT NUMBER: If appropriate, enter the applicable number of the contract or grant under which the report was prepared.

8b. or 8c. PROJECT NUMBER: Enter the appropriate military department identification, such as project number, subproject number, system number, task number, etc.

9a. ORIGINATOR'S REPORT NUMBER(S): Enter the official report number by which the document will be identified and controlled by the originating activity. This number must be printed on this report.

9b. OTHER REPORT NUMBER(S): If the report has been assigned any other report numbers (either by the originator or by the sponsor), also enter this number(s).

10. AVAILABILITY/LIMITATION NOTES: Enter any limitations on further dissemination of the report, other than those

imposed by security classification, using standard statements such as:

- (1) "Qualified requesters may obtain copies of this report from DDC."
- (2) "Foreign dissemination and classification of this report by DDC is not authorized."
- (3) "U. S. Government agencies may obtain copies of this report directly from DDC. Other qualified DDC users shall request through _____."
- (4) "U. S. military agencies may obtain copies of this report directly from DDC. Other qualified users shall request through _____."
- (5) "All distribution of this report is restricted. Classified DDC users shall request through _____."

If the report has been furnished to the Office of Technical Services, Department of Commerce, for sale to the public, indicate this fact and state the price, if known.

11. SUPPLEMENTARY NOTES: Use for additional explanatory notes.

12. SPONSORING AND MILITARY AGENCY: Enter the name of the departmental project office or laboratory sponsoring (paying for) the research and development. Include address.

13. ABSTRACT: Enter an abstract giving a brief and factual summary of the document indicative of the report, even though it may also appear elsewhere in the body of the technical report. If additional space is required, a continuation sheet shall be attached.

It is highly desirable that the abstract of classified reports be unclassified. Each paragraph of the abstract shall end with an indication of the military security classification of the information in the paragraph, represented as (TS), (S), (C), or (R).

There is no limitation on the length of the abstract. However, the suggested length is from 150 to 225 words.

14. KEY WORDS: Key words are technically meaningful terms or short phrases that characterize a report and may be used as index entries for cataloging the report. Key words must be selected so that no security classification is required. Identifiers, such as equipment model designations, trade name, military project code name, geographic location, may be used as key words but will be followed by an indication of technical content. The assignment of links, ranks, and weights is optional.

UNCLASSIFIED

Security Classification